Aus dem Institut für Tierpathologie
des Fachbereichs Veterinärmedizin
der Freien Universität Berlin

In Kooperation mit der
Klinik für Radiologie, Charité – Universitätsmedizin Berlin

Entwicklung und Evaluierung von neuartigen Bildgebungsmodalitäten für die Charakterisierung von abdominalen Aortenaneurysmen im Mausmodell

Inaugural-Dissertation
zur Erlangung des Grades eines
Doktors der Veterinärmedizin
an der
Freien Universität Berlin

vorgelegt von
Dilyana Branimirova Mangarova
Tierärztin
aus Varna, Bulgarien

Berlin 2022
Journal-Nr.: 4344

Aus dem Institut für Tierpathologie

des Fachbereichs Veterinärmedizin

der Freien Universität Berlin

In Kooperation mit der

Klinik für Radiologie,

Charité – Universitätsmedizin Berlin

Entwicklung und Evaluierung von neuartigen Bildgebungsmodalitäten für die Charakterisierung von abdominalen Aortenaneurysmen im Mausmodell

Inaugural-Dissertation

zur Erlangung des Grades eines

Doktors der Veterinärmedizin

an der

Freien Universität Berlin

vorgelegt von

Dilyana Branimirova Mangarova

Tierärztin

aus Varna, Bulgarien

Berlin 2022

Journal-Nr.: 4344

Gedruckt mit Genehmigung

des Fachbereichs Veterinärmedizin

der Freien Universität Berlin

Dekan:	**Univ.-Prof. Dr. Uwe Rösler**
Erster Gutachter:	**Univ.-Prof. Dr. Robert Klopfleisch**
Zweiter Gutachter:	**Prof. Dr. Marcus R. Makowski**
Dritter Gutachter:	**Univ.-Prof. Dr. Heidrun Gehlen**

Deskriptoren (nach CAB-Thesaurus):
mice; animal models; laboratory animals; aorta; aneurysm;
magnetic resonance imaging

Tag der Promotion: 05.04.2022

Declare the past, diagnose the present, foretell the future.

Hippocrates

TABLE OF CONTENTS

LIST OF FIGURES AND TABLES

LIST OF ABBREVIATIONS

^{18}F-FDG	^{18}F-Fluorodeoxyglucose
AAA	abdominal aortic aneurysm
Ang II	angiotensin II
ApoE	apolipoprotein-E
CCL2	CC-chemokine ligand 2
CD68	cluster of differentiation 68
CKD	chronic kidney disease
CT	computed tomography
ECM	extracellular matrix
EVAR	endovascular aneurysm repair
EvG	Elastica van Gieson
FFP	field-free-point
FOV	field of view
HE	hematoxylin and eosin
Hz	Hertz
IF	immunofluorescence
IL	interleukin
ILT	intraluminal thrombus
INFG	interferon gamma
LA-ICP-MS	laser ablation inductively coupled plasma mass spectrometry
MEGs	motion-encoding gradients
miRNAs	micro ribonucleic acids
MMP	matrix metalloproteinase
MNP	magnetic nanoparticles
MPI	magnetic particle imaging

MPS	magnetic particle spectroscopy
MRE	magnetic resonance elastography
MRI	magnetic resonance imaging
PRS	Picrosirius Red
RF	radiofrequency
ROI	region of interest
SMC	smooth muscle cell
SNR	signal to noise ratio
T	Tesla
T1	longitudinal relaxation time
T2	transversal relaxation time
TNFA	tumor necrosis factor alpha
TOF	time of flight
TR	repetition time
US	ultrasound
µmMRE	microscopic multifrequency magnetic resonance elastography

1 INTRODUCTION

1.1 Abdominal aortic aneurysm

This chapter briefly outlines the current state of scientific knowledge with regard to the development, diagnosis and treatment of abdominal aortic aneurysms in humans and elaborates on the animal models of the disease.

1.1.1 Definition, etiology and risk factors

An abdominal aortic aneurysm (AAA) is defined as a weakening of the abdominal portion of the aorta, leading to progressive dilatation and eventually, rupture (Golledge, Muller et al. 2006, Golledge 2019). Consequently, AAAs cause approximately 150,000 - 200,000 deaths per annum (Sampson, Norman et al. 2014, GBD 2013 Mortality and Causes of Death Collaborators 2015).

While there are some distinct causes for AAA development such as trauma, infections (brucellosis, salmonellosis, tuberculosis), inflammatory disease (Takayasu disease, Behçet disease) and connective tissue disorders (Marfan syndrome), most AAAs are considered non-specific (Matsumura, Hirano et al. 1991, Erentug, Bozbuga et al. 2003, Sakalihasan, Limet et al. 2005). Risk factors associated with AAA development are coronary artery disease (Svensjo, Bjorck et al. 2011), hypertension (Svensjo, Bjorck et al. 2011, Patelis, Moris et al. 2017), family history of AAA (Patelis, Moris et al. 2017), atherosclerosis (Patelis, Moris et al. 2017), Caucasian origin (Jahangir, Lipworth et al. 2015) and smoking (Lederle, Johnson et al. 1997, Jamrozik, Norman et al. 2000, Svensjo, Bjorck et al. 2011). It has been hypothesized that the currently decreasing percentage of smokers is directly linked to the declining AAA prevalence in some populations (Lederle 2011, Svensjo, Bjorck et al. 2011). Protective factors for AAA include African or Asian origin (Lederle, Johnson et al. 1997, Jacomelli, Summers et al. 2017) and female gender (Ulug, Powell et al. 2016). While the prevalence in females is significantly lower than in males (Pleumeekers, Hoes et al. 1995), AAAs in females have an overall worse prognosis (Norman and Powell 2007).

There are various definitions of the degree of aortic dilatation that is considered an AAA. It is generally accepted that an AAA has an infrarenal aortic diameter of more than 3 cm (Lederle, Johnson et al. 1997), diagnosed by either ultrasonography (US) or computed tomography (CT). Other common definitions are (1) infrarenal to suprarenal diameter ratio of 1.2 or higher (Alcorn, Wolfson et al. 1996); (2) infrarenal to suprarenal diameter ratio of 1.5 or higher (Moher, Cole et al. 1992); (3) infrarenal diameter of 4 cm or more (Lederle, Johnson et al. 1997); (4) infrarenal aortic diameter that is more than 1.5 times the expected diameter on the basis of body size, sex and age (Lederle, Johnson et al. 1997).

While there is no consensus on AAA measurements, a solid classification on morphological and anatomical criteria of aneurysms exists. An aneurysm with all three arterial layers involved is defined as a *true* aneurysm (Corriere and Guzman 2005). Conversely, a *false aneurysm* or *pseudoaneurysm* consists of an extramural hematoma that is bounded only by the adventitia (Kalapatapu, Shelton et al. 2008). The macroscopic form of an aneurysm is classified as either *fusiform* (spindle-shaped) or *saccular* (spherical, “berry” aneurysm) (Biasetti, Gasser et al. 2010). Besides in the abdominal aorta, aneurysms can form in various other blood vessels in the body, e.g., in the brain (Lawton, Quinones-Hinojosa et al. 2005), kidneys (Henke, Cardneau et al. 2001), legs (Corriere and Guzman 2005) and thoracic aorta (Elefteriades and Farkas 2010). Throughout this work, we use the terms *aneurysm* and *AAA* interchangeably to describe an abdominal aortic aneurysm.

1.1.2 Pathophysiology

The following section focuses on the current understanding behind AAA development in humans. The specifics of murine AAAs can be found in the paragraph entitled *Animal models of abdominal aortic aneurysms*.

There are three main theories on the initiation of AAAs. The most widely supported current theory is based on chronic aortic inflammation and simultaneous degradation of the extracellular matrix (ECM) (Keeling, Armstrong et al. 2005, Hellenthal, Buurman et al. 2009, Golledge 2019). In healthy aortic tissue, a complex network of ECM proteins and fibers is responsible for the mechanical stability during blood pressure fluctuations (Sakalihasan, Limet et al. 2005). Elastin and collagen are the most abundant ECM fibers (Tsamis, Krawiec et al. 2013) with elastin representing up to 30% of the dry weight (Krettek, Sukhova et al. 2003). Tropoelastin is initially secreted by fibroblasts and smooth muscle cells (SMCs) and is then attached onto microfibrills and crosslinked via lysil oxidase, building elastin in its final form (Krettek, Sukhova et al. 2003). The cross-linking between the elastic fibers can be damaged by certain proteases with elastase activity (Sakalihasan, Limet et al. 2005). In aneurysmal aortas, progressive degradation and defective synthesis of elastin occur, leading to decreased overall concentration and functional loss (Sakalihasan, Heyeres et al. 1993, Dobrin and Mrkvicka 1994, Krettek, Sukhova et al. 2003). Collagen, especially type I and III, provides tensile strength and is abundant in the media and in the adventitia (Sakalihasan, Limet et al. 2005). It is thought that the collagen-rich, adventitial tissue is responsible for withstanding a rupture and that collagen degradation is the final step to rupture (Dobrin and Mrkvicka 1994). An increase in collagen turnover has been reported, suggesting that a repair mechanism for collagen degeneration exists (Satta, Juvonen et al. 1995). Therefore, a rupture is thought to occur when the balance between synthesis and degradation is shifted towards the latter (Sakalihasan, Limet et al. 2005). A reduction in medial smooth muscle cell density is also

apparent in AAAs (Lopez-Candales, Holmes et al. 1997). The above described ECM degradation is caused by proteases produced by resident SMCs and fibroblasts as well as inflammatory cell influx from the bloodstream (Sakalihasan, Limet et al. 2005). Matrix metalloproteinases (MMPs) represent a family of zinc-mediated enzymes that can be activated by other proteinases (Ogata, Enghild et al. 1992). It has been demonstrated that MMP-2, -3, -9 and -12 are responsible for AAA initiation and progression by driving elastolysis and collagenolysis in AAAs (Keeling, Armstrong et al. 2005). Elastin degradation and locally released cytokines both act chemotactic to leukocytes, causing even further inflammatory cell recruitment (Koch, Kunkel et al. 1993, Hance, Tataria et al. 2002). The assumption that inflammation plays a major role has been backed by studies analyzing human AAA tissues and focusing on different types of immune cells and mediators. Macrophages and lymphocytes play a substantial role (Davies 1998, Daugherty and Cassis 2002, Ocana 2003). It has been shown that B cells and immunoglobulins infiltrate the AAA and form clusters around small vessel with macrophages and T cells (Furusho, Aoki et al. 2018). Activated T cells, B memory cells and macrophages are the majority of cell types found in the adventitia and outer media (Ocana 2003). Regarding cytokines, it is thought that multiple interleukins (IL), e.g. IL1B, IL6, IL8, prostaglandin E2, tumor necrosis factor alpha (TNFA), interferon gamma (INFG) and CC-chemokine ligand 2 (CCL2), are all upregulated in human AAAs while TNFA, INFG and CCL2 show a level of specificity to AAAs compared to other vascular pathologies (Golledge, Walker et al. 2009). Nowadays it is widely accepted that inflammation plays a crucial role in all types of AAA so that the formerly widespread classification as *inflammatory aneurysm* is now obsolete (Golledge 2019).

The second theory is based on the assumption that atherosclerosis is responsible for aneurysmal development. A large body of literature shows that there is indeed an association between atherosclerosis and AAA, but it remains unknown whether the connection is causal or whether the same risk factors apply to both vascular pathologies (Lederle, Johnson et al. 1997, Singh, Bonaa et al. 2001, Golledge and Norman 2010, Tang, Yao et al. 2016, Yao, Folsom et al. 2018). Similarities in the regions of the aorta that are prone to both diseases support this theory (Xu, Zarins et al. 2001). Additionally, compensatory arterial expansion takes place in atherosclerosis in order to compensate for plaque growth (Ward, Pasterkamp et al. 2000). Thus, some authors suggest that excessive positive arterial remodeling triggers AAA development (Ward, Pasterkamp et al. 2000, Golledge and Norman 2010). An alternative theory, proposed by Golledge and Norman in 2010, suggests that AAAs and atherosclerosis can develop separately and thereupon each condition can potentially trigger the other (Golledge and Norman 2010). The term *atherosclerotic aneurysm* is therefore also outdated (Eiseman and Hughes 1956).

The third theory states that the etiology of AAA is primarily genetic. A Swedish study focusing on AAAs in twins demonstrated that the monozygotic twin of a person with a diagnosed AAA is 71 times more likely to develop an aneurysm in comparison to twins that were both AAA-free (Wahlgren, Larsson et al. 2010). Moreover, first-degree relatives of confirmed AAA patients have an approximately two times higher risk than persons with no family history (Larsson, Granath et al. 2009). This theory was also backed up by a recent genomic meta-analysis by Jones et al., 2016 that found AAA-specific loci and also suggested a central role for MMP9 (Jones, Tromp et al. 2017), leading back to the first theory.

1.1.3 Diagnosis

AAAs are usually asymptomatic and therefore present as an incidental finding during routine abdominal imaging. Screening programs for high-risk populations such as those introduced in some regions of the Australia, Norway, Sweden, United States of America and United Kingdom, might improve earlier diagnosis (Lederle, Johnson et al. 1997, Jamrozik, Norman et al. 2000, Singh, Bonaa et al. 2001, Svensjo, Bjorck et al. 2011, Oliver-Williams, Sweeting et al. 2018). Some patients experience abdominal or back pain, and these AAAs are thought to have a higher risk of rupture in comparison to asymptomatic AAAs (Moll, Powell et al. 2011). If a patient with a previously diagnosed AAA is admitted to a hospital with signs of shock and pain, it is highly likely that the symptoms are linked to a ruptured AAA and they should be directly admitted for surgery without the need of any additional diagnostics (Moll, Powell et al. 2011). For all other patients, the presence and staging of an AAA is performed via diagnostic imaging.

AAAs are usually diagnosed by computed tomography (CT), ultrasound (US), or magnetic resonance imaging (MRI). Based on its high availability, low cost, high accuracy and simple application, ultrasound is as of today (2021) the standard method for AAA imaging (Thompson, Ashton et al. 2009, Hong, Yang et al. 2010). However, the presence of bowel gas or obesity can limit the efficacy of US application (Hong, Yang et al. 2010). CT is often the imaging modality of choice for post-surgery AAAs, since it is highly accurate and reproducible (Nyman and Eriksson 2008), but it comes at the cost of ionizing radiation. In addition, patients with reduced kidney function might develop acute kidney injury following intravenous exposure to iodinated contrast agents. Therefore, MRI is considered a compelling alternative for AAA imaging nowadays as it does not involve ionizing radiation while also being highly reproducible. Moreover, it has been shown that MRI can detect endoleaks that were not visible by CT angiography (Wicky, Fan et al. 2003) and it can also visualize the aneurysmal thrombus in detail (Labruto, Blomqvist et al. 2011). Still, MR imaging is not as widely available as the aforementioned techniques and it comes at a higher cost.

The current clinical AAA staging and decision on surgical repair are calculated based on AAA size on imaging with those larger than 5.5 cm carrying a substantial risk (Lederle, Johnson et al. 2002, Scott, Kim et al. 2005, Moll, Powell et al. 2011). However, AAA size acquisition is not harmonized amongst imaging modalities and there are no reading guidelines, often leading to high variability and under- or overtreatment of patients (Tomee, Meijer et al. 2021). Both the external and the internal aortic diameter could be measured in ultrasonography (Moll, Powell et al. 2011, Oliver-Williams, Sweeting et al. 2018), which accounts for 2 - 5 mm size difference and may cause potential misinterpretations (Moll, Powell et al. 2011). The measurements also vary between different imaging modalities, with CT measurements consistently higher than US measurements in the same patient (Manning, Kristmundsson et al. 2009).

1.1.4 Treatment

Currently, there is no widely accepted pharmaceutical therapy that causes aneurysm growth to cease (Kokje, Hamming et al. 2015). While some therapies such as propranolol (Brophy, Tilson et al. 1988), calcium channel blockers (Takahashi, Matsumoto et al. 2013), angiotensin-converting enzyme inhibitors (Borhani, Lee et al. 2000), platelet inhibitors (Dai, Louedec et al. 2009), antidiabetic drugs (Wang, Guo et al. 2019), statins (Steinmetz, Buckley et al. 2005) and doxycycline (Pyo, Lee et al. 2000) showed promising results in animal models, the translation to a clinical trial was not clearly promising for any of the aforementioned (Kokje, Hamming et al. 2015). One recent clinical trial demonstrated that metformin, an antidiabetic drug leads to decreased AAA enlargement in diabetic AAA patients, yet it remains unknown whether the same effect applies to non-diabetic AAA patients (Itoga, Rothenberg et al. 2019). The Guidelines of the European Society for Vascular Surgery recommends prescribing statins to all patients diagnosed with AAA, since statins reduce the overall risk of cardiovascular diseases (Wanhainen, Verzini et al. 2019). A recent AAA therapy approach that shows positive results in animal models but has not yet been tested in human patients includes different micro ribonucleic acids (miRNAs) and miRNA inhibitors (Maegdefessel, Azuma et al. 2012, Maegdefessel, Azuma et al. 2012, Maegdefessel, Spin et al. 2014).

Since no effective pharmaceutical therapies are available for AAAs, the only effective treatment option is surgical repair (Golledge 2019). Surgical aneurysm repair is recommended for the following aneurysm types: (1) large and asymptomatic; (2) symptomatic, regardless of size; (3) ruptured, regardless of size (Moll, Powell et al. 2011). For patients with small AAAs and those that are unfit for surgery, there are no treatment options available (Golledge 2019). Surgical aneurysm repair can be divided into two main categories: elective and emergency. Regarding elective surgery, the decision on whether to operate or to wait is based on a cost-benefit analysis between aneurysm size, rupture risk and mortality (Moll, Powell et al. 2011). Traditionally, a laparotomy is performed and the aneurysm is replaced by a synthetic graft.

This method is also known as an open repair (Dubost, Allary et al. 1951). The second method available is an endovascular aneurysm repair (EVAR), which relies on an intraluminal stent graft positioned through retrograde cannulation of the femoral artery (Parodi, Palmaz et al. 1991). While the data on EVAR suggests an early survival advantage (Powell, Sweeting et al. 2017), this method still has some considerable disadvantages, e.g. repetitive post-procedure imaging surveillance (Cantisani, Grazhdani et al. 2015), and frequent endoleaks, defined by persistent perfusion of the aneurysmal sac by either arterial side branches or by stent leaks (Cantisani, Grazhdani et al. 2015, Powell, Sweeting et al. 2017). Nonetheless, EVAR is currently the method of choice in many regions of the world when attainable (Townsley, Soh et al. 2021), as it is associated with reduced surgery length, reduced blood loss, trauma, pain, length of hospital stay and requires local anesthesia only (Moll, Powell et al. 2011).

1.1.5 Animal models of abdominal aortic aneurysms

The purpose of studying AAA in animal models is twofold. On one side, the pathology of AAAs is not completely deciphered, so that by varying different factors, both environmental and genetic, the initiating mechanisms of AAA can be analyzed in an experimental setting. On the other side, animal models are used in the search for efficient pharmacological therapies, improved surgical repair techniques and advanced prosthetics (grafts and stents) as well as optimizing imaging techniques in preclinical research. One of the most common rodent AAA models is the angiotensin II (Ang II) - infused Apolipoprotein E deficient ($ApoE^{-/-}$) mouse model. Originally introduced as an atherosclerosis disease model, the development of AAAs in this mouse strain originated as an accidental finding (Daugherty, Manning et al. 2000). This model mimics some important human aneurysm characteristics such as pronounced inflammation and aortic rupture, as well as confounding factors such as smoking (Wang, Zhang et al. 2012) and male sex (Henriques, Huang et al. 2004).

The following paragraph briefly describes the $ApoE^{-/-}$ Ang II AAA mouse model, as employed in our lab. More information about the detailed practical applications of this model is available under *Publication 1* and *Publication 2*. In order to induce an AAA, a surgical implantation of an Ang II-filled osmotic minipump is performed (Lu, Howatt et al. 2015). The osmotic minipump consists of a body and a flow moderator, has a total size of approximately 2 cm, is implanted in the dorsal neck area and is – in our experience – tolerated very well by the animals. The amount of Ang II is calculated individually for each mouse, based on the animal's weight. Combined intraperitoneal anesthesia (500 µg/kg medetomidine, 50 µg/kg fentanyl, and 5 mg/kg midazolam) is applied and once an anesthetic level of surgical tolerance is achieved, a surgical field of approximately 1.5 x 1 cm is prepared by shaving, disinfecting and draping the surrounding area. The pump is then inserted in a subcutaneous pouch in a caudal direction using a hemostat. Lastly, the wound is closed by several (3-5) single absorbable sutures and

the anesthesia is reversed by applying antidotes (2.5 mg/kg atipamezole, 1,200 µg/ kg naloxone, 500 µg/kg flumazenil). After surgery, the development of AAAs expands over 4 weeks. In short, in the first days following implantation of an Ang II-filled minipump, an infiltration of macrophages into the media of the suprarenal aorta occurs; simultaneously, elastin degradation is initiated (Saraff, Babamusta et al. 2003). Subsequently, a medial break leads to extensive lumen expansion and often, thrombus formation (Saraff, Babamusta et al. 2003). While in most mice the adventitia constrains the thrombus, approximately 10% of mice suffer a fatal rupture at this stage (Saraff, Babamusta et al. 2003). This could possibly be explained by the parallel occurring hypertrophy of the adventitia and an imbalance between the medial degradation and the adventitial thickening (Manning, Cassis et al. 2002, Saraff, Babamusta et al. 2003, Trachet, Aslanidou et al. 2017). The formation of the intramural thrombus occurs approximately a week after AAA induction and is accompanied by an inflammatory response and continuous ECM remodeling. Re-endothelialization of the dilated lumen and formation of a “neomedia”, covering the breakage site are often seen (Daugherty, Rateri et al. 2006). Additionally, pronounced neovascularization of the adventitial layer takes place (Saraff, Babamusta et al. 2003).

The following table represents an overview of various techniques and animal models for the induction of AAAs.

Table 1. Animal models of abdominal aortic aneurysms (AAA). *The “✓” symbolizes models that develop AAAs while the “X” represent phenotypes that were shown to be protective for aneurysmal development.*

	Angiotensin II	Cigarette smoke components	Elastase	Calcium chloride	Collagenase	Mechanical & hemodynamic forces	Xeno- and allografts	Aortic injury	Genetic factors only	Dietary alterations	Betaaminopropionitrile	
Mouse												
ApoE$^{-/-}$	✓											(Daugherty, Manning et al. 2000)
ApoE$^{-/-}$ x eNOS$^{-/-}$										✓		(Kuhlencordt, Gyurko et al. 2001)
Blotchy mouse									✓			(Brophy, Tilson et al. 1988)
B6129			✓									(Laser, Lu et al. 2012)
C57BL/6J			✓									(Bhamidipati, Mehta et al. 2012)
C57BL/6J				✓								(Chiou, Chiu et al. 2001)

	Angiotensin II	Cigarette smoke components	Elastase	Calcium chloride	Collagenase	Mechanical & hemodynamic forces	Xeno- and allografts	Aortic injury	Genetic factors only	Dietary alterations	Betaaminopropionitrile	
C57BL/6J	✓										✓	(Kanematsu, Kanematsu et al. 2010)
C57BL/6J			✓								✓	(Lu, Su et al. 2017)
C57BL/6J		✓	✓									(Bergoeing, Arif et al. 2007)
C57BL/6N	✓	✓										(Ji, Zhang et al. 2014)
CD43$^{-/-}$			X									(Zhou, Yan et al. 2013)
IL-17$^{-/-}$			X									(Sharma, Lu et al. 2012)
LDLR$^{-/-}$	✓											(Cassis, Gupte et al. 2009)
MMP9 $^{-/-}$			X									(Pyo, Lee et al. 2000)
pCPB$^{-/-}$			✓									(Schultz, Tedesco et al. 2010)
TIMP$^{-/-}$			✓									(Eskandari, Vijungco et al. 2005)
Tsukuba mouse									✓			(Nishijo, Sugiyama et al. 1998)
129/SvEv		✓	✓									(Buckley, Wyble et al. 2004)
Rat												
Fischer-344 rat							✓					(Allaire, Muscatelli-Groux et al. 2002)
Wistar rat						✓		✓				(Mata, Prudente et al. 2011)
Sprague-Dawley rat						✓						(Tanaka, Zaima et al. 2015)
Rabbit												
New Zealand white rabbit			✓									(Bi, Zhong et al. 2013)
New Zealand white rabbit			✓	✓								(Bi, Zhong et al. 2013)
New Zealand white rabbit			✓			✓						(Bi, Zhong et al. 2015)
Dog												
Beagle			✓									(Boudghène, Anidjar et al. 1993)
Pig												
Unknown race			✓			✓						(Molacek, Treska et al. 2009)
Yorkshire			✓		✓							(Hynecek, DeRubertis et al. 2007)
Unknown race			✓	✓	✓	✓						(Czerski A 2013)
Taiwanese Lanyu minipig						✓						(Lin, Wu et al. 2013)
Unknown race							✓					(Riber, Ali et al. 2017)
Fish												
Zebrafish	✓											(Folkesson, Sadowska et al. 2016)

1.2 Imaging modalities for abdominal aortic aneurysms

This chapter focuses on the underlying theoretical foundations of MRI, magnetic particle imaging (MPI), magnetic particle spectroscopy (MPS), magnetic resonance elastography (MRE) and related contrast agents to facilitate understanding of the relevant concepts introduced in the present work.

1.2.1 Magnetic resonance imaging

MRI represents a non-invasive, radiation-free imaging technique that makes use of magnetism and low-energy radiofrequency signals to obtain images of the body. Generally, an MRI scanner consists of radiofrequency coils for signal generation and transmission, gradient magnets and a main magnet with field strength ranging from 1.5 Tesla (T) for clinical applications to 10.5 Tesla for experimental purposes (Yacoub, Grier et al. 2020).

MRI relies on a quantum mechanics model, illustrating how nuclei spin around their own axes and act as small magnetic dipoles. A proton has a net +1 positive charge and a net unbalanced nuclear spin and therefore, a nuclear magnetic moment. Hydrogen is the most frequently used nucleus for clinical imaging, yet sodium, carbon-13 or phosphorus imaging is also possible (van Geuns, Wielopolski et al. 1999). Normally, the magnetic moments of those nuclei cancel each other out, resulting in a zero net magnetic vector. When an external magnetic field is applied, the nuclei orient either parallel or antiparallel to the external field. The parallel alignment is associated with lower energy and is therefore the preferred positioning, while the antiparallel alignment requires more energy. Under those circumstances, the net magnetization vector results from the difference in both alignments. When aligned with or against the magnetic field the individual nuclei are not motionless, but rather precess around the direction of the external magnetic field. The frequency, at which the precession occurs is defined as the Larmor frequency and is dependent on the strength of the magnetic field and gyromagnetic ratio of the nucleus. Since the net magnetization vector of the nuclei is static, it does not produce any measurable signal. Therefore, radiofrequency (RF) energy pulses equal to the Larmor frequency value are applied. As a consequence, a part of the protons jump from the parallel to the antiparallel, higher energy alignment and are “forced” to precess in phase. The resulting net magnetization now flips 90° from to the transverse plane and induces an alternating current that can be measured by placing a receiver coil in vicinity of the patient. By switching the RF frequency off, protons return to their low energy state, the magnetization decays and the resulting signal also decreases over time. The relaxation time is defined as the time required for the signal to return to equilibrium. There are two independent types of relaxation, namely longitudinal and transverse relaxation. The process of realignment to the external magnetic field after exposure to a 90° RF pulse is defined as the longitudinal relaxation and the time required for this process is defined as T1 relaxation time. On the other hand, the

transverse relaxation represents the loss of phase coherence of the spins. The time required for the transverse relaxation is defined as T2 relaxation. Both the T1 and T2 values of various tissues can differ.

In order to create an MR image out of the received signals, slice selection, frequency and phase encoding are performed. For slice selection, a small superimposed magnetic gradient is added along the magnetic field. Frequency and phase encoding provide information on the individual points within a slice. For phase encoding, a temporary gradient is applied between the RF and the signal readout, resulting in a phase shift of the spin precessing. By switching off the gradient, the spins will precess within the original frequency, yet a small phase change remains. By repeating this process, multiple different phase encodings are acquired. In order to differentiate between pixels with the same phase encoding, frequency encoding is applied.

1.2.2 Magnetic particle imaging

MPI represents a tracer-based imaging modality that quantitatively measures the temporal and spatial distribution of magnetic nanoparticles. First introduced by Gleich and Weizenecker in 2005, this novel, radiation-free imaging method quickly gained momentum and is currently employed in the preclinical imaging of the cardiovascular system (Bakenecker, Ahlborg et al. 2018), various cancers (Billings, Langley et al. 2021), stem cell tracking (Sehl and Foster 2021), theranostics (Tay, Chandrasekharan et al. 2021) and pathologies of the brain (Meola, Rao et al. 2019, Makela, Gaudet et al. 2021). During interventional procedures, it is possible to track instruments, e.g. balloon catheters in real-time by injecting a magnetic particle bolus or, alternatively, by labeling or coating the catheter directly (Haegele, Rahmer et al. 2012). Unlike the current clinical methods in interventional radiology – X-ray fluoroscopy and digital subtraction angiography, MPI does not include any ionizing radiation, which is very advantageous for both patients and medical personnel (Buzug, Bringout et al. 2012).

There are several different types of scanner architectures that have been developed by different research groups across the world. The following text discusses the set-up used in the MPI laboratory at Charité Universitätsmedizin Berlin.

While both MRI and MPI make use of magnetic excitation to create an image, the mechanism behind both modalities differs. As described in the last chapter, conventional MRI relies on nuclear magnetization while MPI employs electron magnetization. The main principle of MPI is to use only the non-linear part of the magnetization answer of magnetic nanoparticles (MNPs) in an oscillating excitation magnetic field. Excited by an external oscillating field (drive field) the MNPs generate a linear part of the magnetization response and a non-linear part by the higher harmonics. MPI and MPS are based on the analysis of these higher harmonics. MPI requires additionally a strong static magnetic gradient field (selection field) to enable the spatial encoding. In the range of this selection field MNP at all positions are in saturation state due to

the high field strength except only the center point, the field-free-point (FFP) where the field strength tends to zero. In the FFP, the magnetic field vanishes. This FFP can be moved by applying three orthogonal drive fields with slightly different frequencies on a Lissajous track in a certain volume (Rahmer, Weizenecker et al. 2009, Rahmer, Weizenecker et al. 2012). During the scan only the MNP at the FFP generate a non-linear magnetization response and become visible by the higher harmonics in the received signal. More details on the technical background of MPI can be found in Rahmer's et al. publications from 2009 and 2012 (Rahmer, Weizenecker et al. 2009, Rahmer, Weizenecker et al. 2012).

The scanner setup is based on a complex coil topology. In a closed-bore scanner, the mouse is positioned in the center of the closed-bore scanner on a tube-like scanning bed. Static and varying magnetic fields are generated by applying direct and alternating currents. Electromagnetic coils are employed for magnetic field generation and for tracer signal reception. The signal transmission setup consists of three types of coils - drive field coils, selection coils and receive coils. In order to visualize 3D distribution, three pairs of drive field and receive coils are needed. The different coil types can be constructed either as dedicated or shared coils. After the raw signal is captured, a reconstruction method is needed to convert the signal into an image. Kaczmarz's algorithm, which is also applied in CT imaging, is used for matrix-based image reconstruction, since it is time and memory effective (Zdun and Brandt 2021). A system matrix serves as a connection between the spatial distribution of the particles and the corresponding Fourier transformed voltage signal. Pre-characterization of the system matrix that involves signal response measurements is required. In short, the system matrix represents a calibration system that analyzes the particle behavior at every position within the scanner.

In comparison to other imaging modalities, MPI exhibits high sensitivity, spatial and temporal resolution (Buzug, Bringout et al. 2012). The magnetization of ultrasmall MNPs in MPI is 10^8 times greater and the relaxation time is 10^4 faster compared to the proton magnetization and T1 relaxation of water in a 1.5 T MRI scanner (Goodwill, Tamrazian et al. 2011). Taken together, these effects translate into a superb signal-to-noise ratio (SNR). The exceptional temporal resolution is illustrated in a study by Weizenecker et al., in which they imaged a beating mouse heart and could trace the movement of the magnetic nanoparticles through the cardiovascular system (Weizenecker, Gleich et al. 2009). In respect to spatial resolution, 1 mm has been accomplished (Gleich and Weizenecker 2005). Moreover, the strength of signal in MPI is proportional to the concentration of nanoparticles, so it is possible to perform quantitative analysis based on this data. In addition, MPI has no depth attenuation and no background signal which are both key features for angiography (Saritas, Goodwill et al. 2013). Since animal tissue is diamagnetic, it does not generate any signal in MPI and appears transparent. Based on this principle, arterial narrowing, dilatations and blockages can be

visualized. This can even be performed real time and in 3D, which is one of the most important advantages of MPI (Buzug, Bringout et al. 2012). Another benefit of MPI is that it is safe for chronic kidney disease (CKD) patients. MRI- and X-ray contrast agents often contain gadolinium or iodine, respectively, both of which could be problematic for patients suffering from CKD (Broome 2008, Goldfarb, McCullough et al. 2009). Ferumoxytol, a clinically approved MNP, is even currently prescribed for anemia treatment in CKD patients (Lu, Cohen et al. 2010). More in-depth information on MRI/MPI tracers can be found in the following chapter.

1.2.3 Magnetic nanoparticles for MRI and MPI

In recent years, the application of nanoparticles, usually defined as particles ranging from 1 to 100 nm (Bakenecker, Ahlborg et al. 2018), has been on the rise in various fields of research, ranging from thermo-therapeutic cancer treatment to cell separation for biotechnological purposes (Tartaj, Morales et al. 2003). For the purpose of MPI, iron oxide nanoparticles with a single domain magnetic core are used (Buzug, Bringout et al. 2012).

These superparamagnetic iron oxide particles are non-toxic (Schneider and Lüdtke-Buzug 2012), have a long history of application as MRI contrast agents and are therefore partially commercially available. The safety application margin of MNPs is quite broad and only a significant overdose of the tracer would lead to iron-overload-related toxic effects (Panagiotopoulos, Duschka et al. 2015). Furthermore, MPI has higher sensitivity which means that smaller amounts of tracer are sufficient to achieve adequate images. While the sensitivity of MRI lies around 50 µmol(Fe)/L regardless of voxel size, in MPI it varies between 13 nmol(Fe)/L for a 1mm^3 voxel and 13 pmol(Fe)/L for a 1 cm^3 voxel (Gleich 2013). Most MNPs magnetic core consists of a mixture of magnetite (Fe_3O_4) and maghemite (Fe_2O_3), coated with dextran, polyethylene glycol, silica, chitosan to prevent agglomeration and improve their physicochemical stability (Buzug, Bringout et al. 2012). In addition, the surface can be functionalized by adding ligands, e.g. antibodies to allow for highly sensitive interactions within biological systems (Wu, Su et al. 2020). Particles that have a magnetic core of around 30 nm seem to be ideal for MP imaging (Gleich and Weizenecker 2005). Because of their superparamagnetic nature, they show no remnant magnetization in the absence of an external magnetic field. After injection, iron oxide nanoparticles are eliminated in the same route as endogenous iron (Panagiotopoulos, Duschka et al. 2015). Most of the iron is deposited as ferritin, an iron storage protein that is highly concentrated in reticuloendothelial system (RES) tissues such as liver, spleen, lymph nodes or bone marrow (Panagiotopoulos, Duschka et al. 2015). MNP tracers are widely available, easy to handle and less costly than radionuclides (Wu, Zhang et al. 2019). While some research groups develop their own, optimized MNPs,

others rely on commercially available ones such as Resovist, Ferumoxytol, Synomag or Perimag (Kaul, Mummert et al. 2017, Kratz, Taupitz et al. 2018, Liu, Chiu-Lam et al. 2021).

In regard to MRI, MNPs have the ability to shorten T2 relaxation times and are therefore used as negative contrast agents (Bulte and Kraitchman 2004). In clinical MRI examinations, MNPs are often used for liver imaging, since healthy liver tissue contains abundant phagocytic cells that take up the MNPs, while pathologically altered areas show reduced uptake (Bulte 2019). While MNPs represent effective contrast agents with a good safety spectrum, they have some major drawbacks. First, MNPs are eliminated rapidly from the bloodstream, which can be unfavorable for some applications (Bulte 2019). Second, since MNPs yield negative contrast, it is difficult to distinguish the source of the produced signal. Other potential sources of “black holes” in MRI are hemorrhages, trapped air and motion artifacts. In addition, MNPs are detected indirectly by their influence on proton relaxation and, therefore, it is not possible to assess the tissue concentration quantitatively (Bulte 2019). The abovementioned disadvantages of MRI are non-existent when the same particles are applied in MPI, since it causes positive contrast, has no background signal (Saritas, Goodwill et al. 2013) and can differentiate between exogenous and body iron, as discussed in detail in the last chapter.

While the term *contrast agent* is usually applied for MR imaging and *tracer* is more common for PET and SPECT, the current work views both terms as synonyms. On the one hand, the same particles that are applied as MR *contrast agents* can be adopted for MPI. However, MPI yields no background signal and therefore, there is no existing contrast between two signal intensities to be compared. On the other hand, a *tracer* is usually associated with nuclear imaging, yet magnetic particles are non-ionizing. Because of these discrepancies, we use both synonymously.

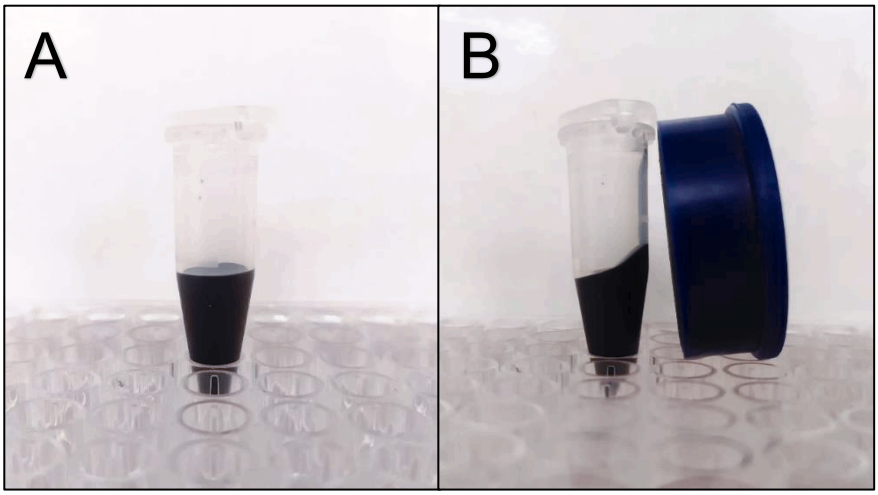

Figure 1. A visual representation of the magnetic properties of MNPs

***A**. MNPs without the influence of an external magnetic field. **B**. MNPs in the vicinity of a small magnet (blue).*

1.2.4 Magnetic particle spectroscopy

Magnetic particle spectroscopy (MPS) can be described as a zero-dimensional magnetic particle imaging without spatial resolution. MPS is often applied as a prerequisite for identifying suitable particles for MP imaging by studying their magnetic spectrum, therefore both methods share the same physical principles. A magnetic particle spectrometer specifically detects the non-linear magnetic response of magnetic nanoparticles in an oscillating magnetic field. The magnetic responses contain both the driving field frequency and the harmonic frequencies that can be separated by filtering. By calibrating the measurements, quantitative comparisons of samples in different environments can be assessed. An internal Fourier transformation of the detected signal is performed. For the measurements, the sample is placed in a PCR tube in the pick-up coil of the MPS system and the non-linear magnetization is collected by a receiver coil. The relaxation processes are dependent on the physical conditions of the sample, e.g. temperature, viscosity and binding state, therefore standardization of the experimental conditions is of high importance.

1.2.5 Magnetic resonance elastography

The mechanical properties of pathologically altered tissues often differ from those of healthy ones (Sarvazyan 1998). Historically, palpation has been used for centuries in the detection of pathological masses in the thyroid, breast or prostate (Muthupillai and Ehman 1996). MRE represents a novel noninvasive phase-contrast MR-based imaging modality for quantitative assessment of the mechanical properties of tissues, based on the propagation of shear waves.

MRE has several advantages compared to other medical imaging techniques. Colloquially titled “palpation imaging” (Muthupillai and Ehman 1996), MRE permits mechanical quantification of body regions that are otherwise inaccessible to the physician’s hand without surgery. While MRI detects the magnetic relaxation of tissues, X-ray/CT characterize tissue radiation absorption and ultrasound measures acoustic echogenicity, none of those imaging modalities is capable of assessing the mechanical properties of biological tissues. In addition, the elastic modulus of tissue has a wider range of variability (over four orders of magnitude) in comparison to tissue measurements acquired by MRI, CT and US (Manduca, Oliphant et al. 2001, Mariappan, Glaser et al. 2010). The expansive spectrum of MRE tissue values compared to other imaging modalities allows for a more sensitive depiction of pathological alterations.

Since most animal tissues are neither completely solid nor completely liquid, they are best described using the concept of viscoelasticity (Manduca, Oliphant et al. 2001). The governing variable of MRE imaging is the elastic modulus, which is defined as the relationship between stress and strain. In other words, the elastic modulus describes an object’s ability to sustain its original size and shape when subjected to deforming. Shear stiffness is used in MRE as an

approximation for the effective shear modulus at a specified frequency (Low, Kruse et al. 2016). Images of tissue stiffness are therefore often titled stiffness maps or elastograms.

The simplified set up of MRE is as follows: 1) a known cyclic mechanical stress is applied; 2) the mechanical deformation is measured; 3) an elastic modulus is calculated (Muthupillai and Ehman 1996, Tzschatzsch, Guo et al. 2016, Hirsch, Braun et al. 2017). MRE can be implemented both on standard 1.5 T or 3T clinical MRI scanners as well as on experimental animal MRI devices. Mechanical excitations can be produced by pneumatic, electromagnetic, acousto-mechanic or piezoelectric actuator devices (Low, Kruse et al. 2016). When the waves propagate through tissue, they cause cyclic spatial displacements (Muthupillai and Ehman 1996). Expected wavelengths can be matched to the field of view (FOV) to ensure acquisition (Manduca, Bayly et al. 2020). In order to further improve the stability and reliability of the acquired data, multiple vibration frequencies can be acquired (Sack, Beierbach et al. 2009). The mechanical waves propagating through the tissue are calculated as a phase shift caused by the cyclic motion of the spins and the displacement at each voxel is measured. By integrating an additional modified phase-contrast imaging sequence in the MR imaging protocol, it is possible to measure the displacement patterns created by propagating shear waves within the tissue of interest. This MRE sequence is based on a conventional MR imaging sequence with additional motion-encoding gradients (MEGs). The MEGs can be applied along all three planes of motion in order to capture the entire 3D wave vector. The MEGs and mechanical excitations are usually synchronized by trigger pulses. Manipulation of the trigger pulse is used to cause a small delay, known as a phase offset. By varying the phase offset between the actuator and the MEGs, multiple wave images (4-8) are acquired (Low, Kruse et al. 2016). Two types of raw images that give information about the shear wave progression are obtained, namely magnitude and phase images. In the phase images, the signal from each pixel represents the displacement vector in the measured direction. The data is then converted into stiffness maps by calculating the wave speed per pixel using an inversion algorithm (Tzschatzsch, Guo et al. 2016, Bertalan, Guo et al. 2019).

So far, MRE has been applied to quantify various healthy and diseased organs and tissues ranging from skeletal muscle (Ringleb, Bensamoun et al. 2007), breast (Patel, Samreen et al. 2021), brain (Di Ieva, Grizzi et al. 2010), liver (Hoodeshenas, Yin et al. 2018), spleen (Yoon, Shin et al. 2019), kidneys (Zhang, Zhu et al. 2018), uterus (Zhang, Long et al. 2021), lungs (McGee, Hubmayr et al. 2009), aorta (Khan, Fakhouri et al. 2018), to prostate (McGrath, Lee et al. 2017). The first clinical application of MRE is the detection and staging of liver fibrosis, which is highly reproducible and currently implemented in many hospitals around the world (Shire, Yin et al. 2011, Low, Kruse et al. 2016).

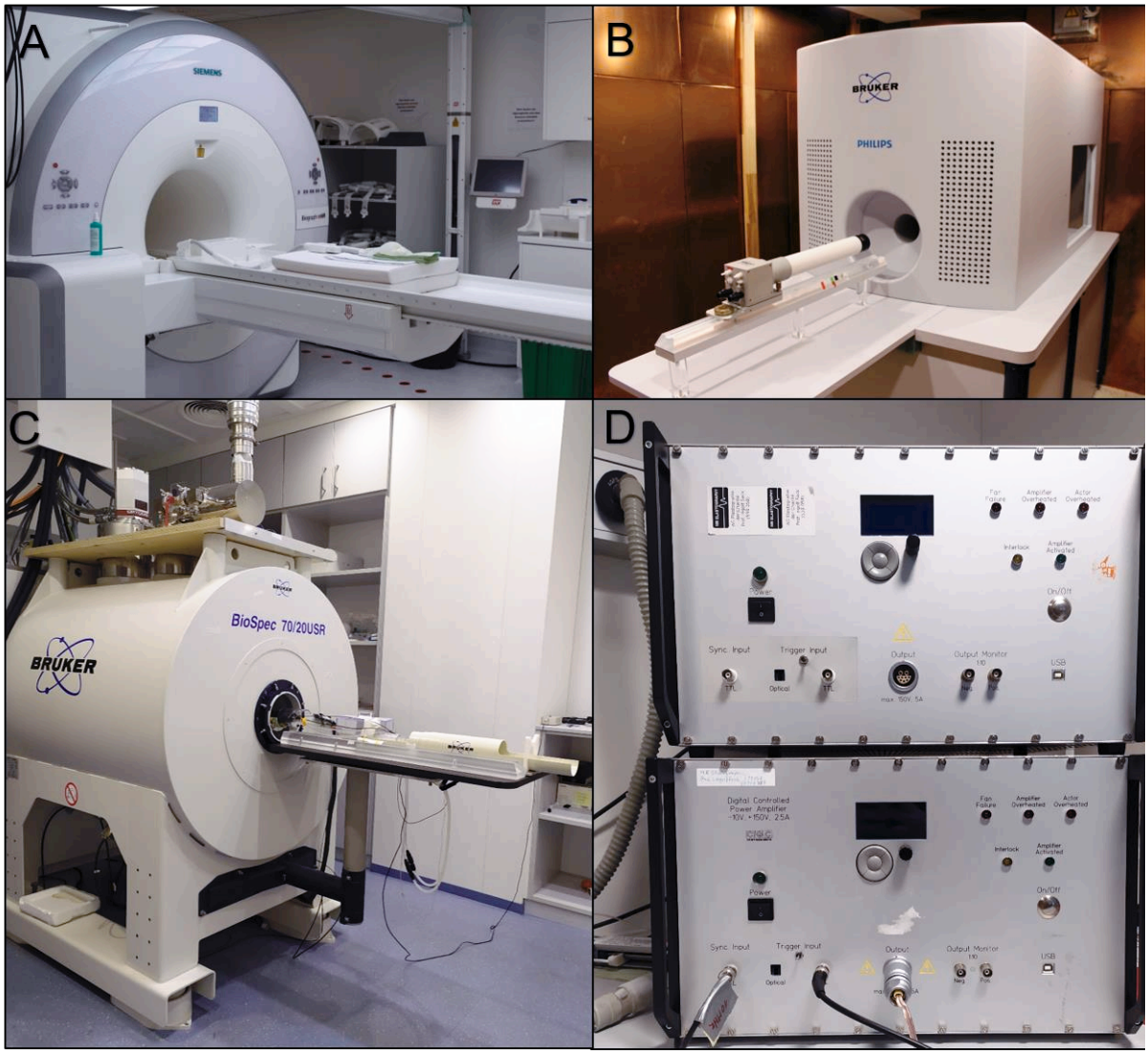

Figure 2. An overview of the imaging devices used in this study

***A**. Clinical 3T magnetic resonance imaging scanner. **B**. Magnetic particle imaging scanner, **C**. Preclinical 7T magnetic resonance imaging scanner. **D.** External magnetic resonance elastography driver device.*

2 AIMS AND OBJECTIVES

The objective of the current work is to assess novel imaging modalities for AAAs in a murine model, by testing following hypotheses:

1) Magnetic resonance elastography allows us to reliably image AAAs and characterize extracellular matrix changes in the aneurysmal thrombus.

2) Magnetic particle imaging enables the visualization and quantification of iron oxide nanoparticles in AAAs, which in turn reflects the degree of inflammation.

3 PUBLICATION I

Title: Microscopic multifrequency magnetic resonance elastography of *ex vivo* abdominal aortic aneurysms for extracellular matrix imaging in a mouse model

Authors: Dilyana B. Mangarova, Gergely Bertalan, Jakob Jordan, Julia Brangsch, Avan Kader, Jana Moeckel, Lisa C. Adams, Ingolf Sack, Matthias Taupitz, Bernd Hamm, Marcus R. Makowski, Jürgen Braun

Year: 2021

Journal: Acta biomaterialia (Vol. 140, Pages 389-397)

Impact factor: 8.947

DOI: https://doi.org/10.1016/j.actbio.2021.11.026

Authors' contribution: I was responsible for the conception and design of the study by developing the theory and planning the experimental setup in detail. I performed the animal experiments and histological analysis of the samples, participated in the MRE measurements and contributed to the interpretation of the MRE data. I also wrote the main body of the manuscript in consultation with all other authors. All authors discussed the results and contributed to the final version. A detailed list of the contributions of the other authors is available in the published version of the paper.

You need to read this publication online.

4 PUBLICATION II

Title: *Ex vivo* magnetic particle imaging of vascular inflammation in abdominal aortic aneurysm in a murine model

Authors: Dilyana B. Mangarova, Julia Brangsch, Azadeh Mohtashamdolatshahi, Olaf Kosch, Hendrik Paysen, Frank Wiekhorst, Robert Klopfleisch, Rebecca Buchholz, Uwe Karst, Matthias Taupitz, Jörg Schnorr, Bernd Hamm, Marcus R. Makowski

Year: 2020

Journal: Scientific reports (*Sci Rep* 10, Article number: 12410)

Impact factor: 4.379

DOI: https://doi.org/10.1038/s41598-020-69299-y

Authors' contribution: I was responsible for conceiving and planning the experiments. I performed the histological analysis of the samples, evaluated the MRI data and participated in the MPI and MPS measurements. I contributed to the analysis of the MPI and MPS data and wrote the main body of the manuscript in consultation with all other authors. All authors discussed the results and contributed to the final version. A detailed list of the contributions of the other authors is available in the published version of the paper.

You need to read this publication online.

5 DISCUSSION

5.1 Imaging ECM remodeling within the aneurysmal thrombus with MRE

MRE represents a promising novel imaging modality that can noninvasively deliver information about the biomechanical constitution of tissue. This could be especially invaluable in AAA imaging, since ECM remodeling influences the stability of the aorta (Dobrin and Mrkvicka 1994). The presented results strongly indicate that MR elastograms can reliably depict the spatial distribution and concentration of ECM proteins in the aneurysmal thrombus.

Elastin and collagen are two of the main ECM components and make out approximately 50% of the dry weight of large human arteries (Harkness, Harkness et al. 1955). Therefore, it is unsurprising that both proteins play a major role in the development of AAAs. Elastin – as the name suggests, provides elasticity and contributes to aortic expansion during systole and recoil during diastole (Wagenseil and Mecham 2009). Conversely, collagen is responsible for the tensile strength of the arterial wall and maintains the structural integrity of the vessel during pressure changes (Wagenseil and Mecham 2009). Normally, ECM remodeling is essential for development and tissue homeostasis, however in the case of AAA it becomes dysregulated and excessive. Elastolysis results in a shift of mechanical stress from the elastic lamellae to collagen fibers, which are 100 to 1000 times stiffer than elastin (Wagenseil and Mecham 2012). As a result of aging and tissue injury, elastin is replaced with collagen since elastin expression is mostly supressed in adult mammals (Wagenseil and Mecham 2012). In addition, non-enzymatic irreversible glycation of long-lived collagen and elastin, also known as advanced glycation end products (AGEs) can also cause stiffening of the arterial wall (Lee and Cerami 1992, Verzijl, DeGroot et al. 2000, Bailey 2001). The resulting ECM proteins are less susceptible to hydrolytic turnover and are stiffer than regular collagen or elastin (Lee and Cerami 1992, Winlove, Parker et al. 1996, Konova, Baydanoff et al. 2004, Diez 2007). Previous studies from our working group resonate with the current results, showing that decreased levels of elastin could cause rupture (Brangsch, Reimann et al. 2019). Furthermore, our findings resonate with those of Dong et al who report a significant decrease in elastin density in a porcine MRE model (Dong, Russell et al. 2020).

The role of collagen in the pathophysiology of AAA is not yet completely deciphered – while some studies support our results and show a lower collagen content in AAA (McGee, Baxter et al. 1991), others show no difference (Gandhi, Irizarry et al. 1994) or even a higher collagen content (Menashi, Campa et al. 1987) compared to a healthy artery. It is possible that these differences arise from the lack of standardization of sample acquisition, measuring methods and protocols or from age differences. Following the ECM remodelling theory, collagen content might also fluctuate during AAA progression due to neosynthesis (Satta, Juvonen et al. 1995)

with rupture occuring when the balance is shifted towards collagenolysis (Sakalihasan, Limet et al. 2005).

Another important factor in the pathology of AAAs is the presence of an aneurysmal thrombus. In humans, the intraluminal thrombus is an active and complex biological entity and its influence on AAA rupture has been studied with great interest over the last decades. ILTs act as a source of proteases (Fontaine, Jacob et al. 2002) and can appear quite heterogenous, demonstrating either distinct layers with varying consistency and microstructure or no apparent organization (Tong, Cohnert et al. 2011, Barrett, Cunnane et al. 2018, Leach, Kao et al. 2019). According to Adolph et al., the ILT is crossed by a continuous network of endothel-lacking cavities, also known as canaliculi (Adolph, Vorp et al. 1997). In this regard, our findings are consistent with previous publications on both human and animal AAAs and highlight the translational potential of the Ang II - infused murine model (Klink, Heynens et al. 2011).

The morphology and structure of the thrombus in turn affect the biomechanical characteristics of the aneurysm wall. A more compliant ILT results in higher wall stress than a less compliant ILT and vice versa: a stiffer ILT leads to a more pronounced reduction in wall stress (Riveros, Martufi et al. 2015). However, the wall under a newly formed, soft, more compliant and not extensively remodeled thrombus might be stronger than the wall under an older ILT (Riveros, Martufi et al. 2015). In other words, the protective biomechanical characteristics that a thick ILT offers by lowering wall stress are canceled out by the weakening of the AAA wall (Haller, Crawford et al. 2018). The ILT-covered wall is thinner and demonstrates signs of inflammation, ECM degradation and SMC apoptosis more frequently (Kazi, Thyberg et al. 2003). Moreover, ILTs with large pores, fissures and cracks result in an increased wall stress compared to non-fissured ILTs (Polzer, Gasser et al. 2011). This is also reflected in *ex vivo* biomechanical testing on human AAA specimen, demonstrating that well organized thrombotic tissue reduces the effects of pressure load on the aneurysmal wall (Di Martino, Mantero et al. 1998). Future studies focusing on longitudinal *in vivo* AAA tracking would be beneficial to study the mechanisms discussed above in a biological system.

So far, the applications of vascular MRE have been demonstrated in normotensive, hypertensive and aneurysmal aortas of humans and swine (Kolipaka, Woodrum et al. 2012, Xu, Chen et al. 2013, Kolipaka, Illapani et al. 2016, Dong, Mazumder et al. 2017, Schaafs, Schrank et al. 2020). To the best of our knowledge, Kolipaka et al. (2016) were the only group to report on the role of thrombi in the context of AAA (Kolipaka, Illapani et al. 2016). However, only the impact of the amount of thrombus on the overall aortic stiffnes was analyzed and no input on the morphology or biomechanics of the thrombus itself were provided.

The limitations of our study are mainly related to the *ex vivo* experimental set up. A detailed depiction can be found in the published version of the paper. Due to the small body size and multiple confounding factors, e.g. movements of the aorta during the cardiac cycle, diminuitive thickness of the aorta, high pulse rate, difficulty to construct a reliable set-up, it was not possible to accurately image the wave propagation in the aneurysm *in vivo*. In addition, increasing the number of mice involved in the study would boost the statistical power of our data.

5.2 Imaging inflammation with MPI

The second key process in the aneurysmal development besides ECM degradation is inflammation. Chronic aortic inflammation leads to ECM degradation and SMC apoptosis as a result of inflammatory cell influx and the release of a wide range of proteolytic enzymes (Golledge 2019). Especially macrophages and monocyte recruitment appear to play a major role in AAA inflammation (Temme, Yakoub et al. 2021). We demonstrated that MNPs taken up by resident macrophages can be used as a surrogate marker of inflammation for MP imaging of AAAs.

AAA development in humans involves a variety of inflammatory cells with macrophages and lymphocytes being more abundant than mast cells and neutrophils (Koch, Haines et al. 1990, Curci, Liao et al. 1998, Daugherty and Cassis 2002, Galle, Schandene et al. 2005, Tsuruda, Kato et al. 2008). Macrophages release a variety of proinflammatory cytokines such as TNFA, IL1B, IL6, as well as MMPs that contribute to ECM degradation (Pearce, Sweis et al. 1992, Szekanecz, Shah et al. 1994, Sakalihasan 1996). Phagocytic cells are recruited to injury sites by different chemokines and degraded ECM, leading to a positive feedback loop and chronic inflammation (Dale, Ruhlman et al. 2015). Since macrophages display plasticity, they can polarize to various phenotypes. The M1 phenotype represents the classical activation cascade and is responsible for the induction of tissue degradation by pro-inflammatory cytokine production (Dale, Ruhlman et al. 2015). Contrarily, M2 macrophages are implicated in tissue repair and inflammation resolution. Therefore, it is possible that an AAA occurs when there is an imbalance between M1 and M2 type macrophages (Dale, Ruhlman et al. 2015).

The role of inflammation in murine AAAs is comparable to that in humans. In rodent AAAs, both the innate and the adaptive immune system are involved in the pathogenesis of aneurysm development (Daugherty, Manning et al. 2000, Steinmetz, Buckley et al. 2005, Bergoeing, Arif et al. 2007, Wang, Zhang et al. 2012, Trachet, Piersigilli et al. 2016, Lu, Su et al. 2017, Trachet, Aslanidou et al. 2017). Conversely, modification of both the innate and adaptive immunity towards downregulation of aortic degradation has been shown to limit AAA development and progression. Meng *et al.* demonstrated that regulatory T cells dose-dependently inhibit the formation of AAAs in an Ang II-infused murine model by decreasing the levels of oxidative

stress, apoptosis, proinflammatory cytokines and MMPs while simultaneously increasing the expression of IL10 and TGF-β (Meng, Yang et al. 2014). In regard to innate immunity, it has been shown that inhibition of mast cell degranulation also lead to reduced AAA development (Tsuruda, Kato et al. 2008). Furthermore, neutrophil depletion also resulted in AAA attenuation in a mouse model (Eliason, Hannawa et al. 2005). In spite of this, several clinical trials showed that anti-inflammatory drugs were unsuccessful in preventing AAA progression (Lindeman, Abdul-Hussien et al. 2009, Meijer and Stigmen 2014, Sillesen, Eldrup et al. 2015). Future studies need to investigate the exact biochemical pathways involved in AAA inflammation to identify possible effective pharmacological therapies.

The feasibility of MNPs as a surrogate marker for AAA imaging has already been demonstrated by MRI in both animal and human studies (Turner, Olzinski et al. 2009, MA3RS Study Investigators 2017). In MRI, MNPs cause shortening of the signal T2/T2* relaxation time which translates in a signal void in the corresponding region. A recent prospective clinical study suggested that AAA expansion rate and risk of clinical events could be predicted via MNP-enhanced MRI (MA3RS Study Investigators 2017). Although the authors administered another type of MNP, namely ferumoxytol, similar results can be expected with ferocarbutran. To our knowledge, we were the first to test feasibility of MPI for imaging inflammation in AAAs. Ferocarbutran was taken up by macrophages in the aneurysmal wall in high enough numbers to produce abundant signal in MPI and MPS 24 hours after injection. In comparison to MRI, MPI has superior sensitivity (Buzug, Bringout et al. 2012) and does not visualize endogenous iron (Wu, Zhang et al. 2019), therefore it can be expected that AAA expansion and potential rupture could be predicted even more reliably with MPI than with MRI.

While many MPI-suitable MNPs are licensed as MRI contrast agents or are being used off-label as such, there are still some concerns that should be addressed by future studies. Even though it is widely accepted that iron oxide nanoparticles have an overall good safety profile, they are still considered foreign bodies by the immune system and can potentially cause immunosuppression, immune stimulation or hypersensitivity reactions in rare cases (Dobrovolskaia, Shurin et al. 2016, Shah and Dobrovolskaia 2018, Geppert and Himly 2021).

Our work has two main limitations. First, the *shadowing effect* of the liver hindered us from imaging the aorta *in vivo*. When two objects with a large difference in their iron content present in the FOV simultaneously, the object containing less iron is suppressed and cannot be imaged (Knopp, Gdaniec et al. 2017, Kratz, Mohtashamdolatshahi et al. 2019). This effect is observed with the suprarenal portion of the aorta, which lies in proximity to the liver in the abdominal cavity. Second, *ex vivo* imaging might cause changes in the MPI signal compared to *in vivo* measurements. This is due to Néel and Brownian particle relaxation mechanism that are both

dependent on viscosity (Zhou, Tay et al. 2018), which in turn can be influenced by the temperature and aneurysmal environment.

5.3 The future of AAA imaging

In spite of major advancements of the scientific knowledge on AAA pathophysiology, the 5.5 cm size criterion still dictates the decision-making regarding surgical intervention (Scott, Kim et al. 2005, Moll, Powell et al. 2011). It is accepted that rupture risk is associated with diameter, with AAAs larger than 5.5 cm carrying a substantial risk (Lederle, Johnson et al. 2002) that increases even further when AAAs expand more (Parkinson, Ferguson et al. 2015). In addition, the aneurysm annual growth rate also appears to be significantly associated with clinical events (Thompson, Cooper et al. 2010). While it is generally thought that small aneurysms are not prone to rupture, some small aneurysms in fact suffer a rupture and some larger ones remain stable (Thompson, Geraghty et al. 2002, Moll, Powell et al. 2011, Kent 2014). Thus, using one single criterion for evaluating a pathology this complex seems somewhat simplistic. Developing new methods for characterizing both the anatomical appearance of aneurysms, and detecting ECM changes and inflammatory markers would help gain more complex insights on rupture risk and make better informed decisions on surgical repair.

Since MRE can be added to virtually any commercial MRI system, the technical implementation for future clinical application would be unproblematic. This was already demonstrated for clinical liver fibrosis MRE (Shire, Yin et al. 2011, Low, Kruse et al. 2016). In addition, since the elastographic measurements are integrated in the MR imaging procedure, a substantial increase in both examination time and cost should not be expected. Unlike some other organs e.g. liver or breast, taking a biopsy is not a feasible option for AAAs. Therefore, it is even more important to have reliable data about the mechanical characteristics in order to better plan and execute a potential surgical AAA repair. The feasibility of MRE for the surveillance of liver transplant patients has been demonstrated recently (Singh, Venkatesh et al. 2016). It would be interesting to see whether this can also be applied for post-surgery AAA surveillance, more precisely for detailed imaging of endoleaks. As most MRE methodologies utilize an external excitation unit that is applied on the skin surface, it is difficult to examine tissues that are located very deep in the body, since part of the kinetic energy is lost in the viscosity and the wave amplitude is attenuated over long distances (Tse, Janssen et al. 2009). Accordingly, MRE imaging of the aorta is a tradeoff between spatial resolution and distance.

In regard to MPI, the current state of development can be compared to that of MRI in the 1980s (Saritas, 2013). Even though the basic physics behind MRI and MPI differ, it is feasible to create a dual-imaging scanner by adapting the same coils for generating the MRI B_0 field and the MPI selection field and for receiving both generated signals (Franke, Heinen et al. 2016). Since there are no fundamental hardware or physics limitations that prevent the construction

of a bigger MPI scanner, it is only a matter of time, engineering and research to create a large scale clinical scanner (Borgert, Schmidt et al. 2013). The first bimodal MPI-MRI tomographic devices are currently being investigated (Franke, Heinen et al. 2013, Vogel, Lother et al. 2014). Alternatively, a shuttle system can be constructed where the patient is transferred on the same imaging bed from an MRI to an MPI scanner that are housed in the same room (Knopp, Gdaniec et al. 2017), similarly to the early PET/CT and PET/MRI imaging developments. Since no ionizing radiation is involved, MPI would be especially useful in cases where routine imaging is required. Nevertheless, the possibility of overheating needs to be further analyzed and technical advancements need to take place in order to visualize larger body areas (Knopp, Gdaniec et al. 2017). The potential applications of MPI for AAA imaging is twofold. On one side, angiographic “first pass” MPI allows visualizing the circulating MNPs and the level of lumen dilatation in 3D. The practicability of this approach was verified in a phantom hemodynamics model (Sedlacik, Frolich et al. 2016) and in an *in vivo* angiography model of healthy rat aortas (Mohtashamdolatshahi, Kratz et al. 2020). On the other side, by imaging the same patient 24 hours later when MNPs have undergone extravasation and accumulation in the AAA, we can indirectly determine the level of inflammatory activity.

5.4 The translational potential of the ApoE$^{-/-}$ mouse model

The knowledge of the pathophysiological development of human AAAs at different disease stages is limited by the fact that tissue samples are available only at the time of surgery or from postmortem examinations, when aneurysms are usually matured. Therefore, no “baseline” data is available. Human AAAs present with a significant decrease in medial SMCs caused by apoptosis (Lopez-Candales, Holmes et al. 1997), distortion and reduction of medial ECM fibers (Lopez-Candales, Holmes et al. 1997) as well as inflammatory cell influx (Koch, Haines et al. 1990). All of those characteristics are mirrored by the Ang II–infused ApoE$^{-/-}$ mouse model employed in the current work. Nonetheless, there are several important differences between human and murine AAAs that should be mentioned.

First, while humans mostly develop infrarenal AAAs (Golledge, Muller et al. 2006), the location in ApoE$^{-/-}$ mice is the suprarenal aorta. The reason for this difference and the specific mechanism for formation in those localizations of the aorta remains widely unknown. Some authors hypothesize that murine Ang II–induced AAAs develop in the suprarenal aorta because this region has a higher degree of curvature (bending) (Goergen, Azuma et al. 2011). In regards to human AAA location, it is possible that the decreased elastin to collagen ratio in the infrarenal aorta is responsible for the predisposition to aneurysm development (Halloran, Davis et al. 1995). To the best of our knowledge, there is no similar characterization study for murine aortas. It remains unclear whether the different anatomical locations mirror different AAA initiation mechanisms in terms of hemodynamics.

Secondly, a growing body of literature argues that the Ang II-infused mouse model represents a pseudoaneurysm and not a true aneurysm, since it essentially develops encapsulated extramural thrombi (Jiang, Jones et al. 2007). In other words, it mimics an aortic dissection rather than an aortic aneurysm (Trachet, Aslanidou et al. 2017). This is illustrated by the terminology of *intraluminal thrombi* in humans opposing to *intramural thrombi* in mice (Busch, Bleichert et al. 2021). To the extent of our knowledge, Ang II-infused models are the only murine models that systematically develop thrombi with demonstrated biological activity. While this partially applies to the combined elastase-BAPN mouse model as well, only half of those animals develop a thrombus and there is no data about the biological activity of the latter (Lu, Su et al. 2017, Busch, Bleichert et al. 2021). In contrast, over 90% of human AAAs exhibit thrombus formation and there is abundant information on the molecular components involved (Lukasiewicz, Reszec et al. 2012, Sakalihasan, Michel et al. 2018). Additionally, human aneurysms also show intramural hemorrhage in some cases, similarly to those exhibited in our mouse model (Busch, Bleichert et al. 2021). Therefore, even though there are histological discrepancies between human and $ApoE^{-/-}$ aneurysms, we believe that they represent a reliable disease model for studying the main pathological characteristics of AAAs.

6 SUMMARY

Development and evaluation of novel imaging modalities for the characterization of abdominal aortic aneurysms in a mouse model

An abdominal aortic aneurysm (AAA) is defined as a permanent local dilatation of the abdominal aorta, usually accompanied by thrombus formation. Once ruptured, an AAA is associated with an overall mortality rate of over 90%. Even though AAAs represent one of the leading causes of sudden death in developed countries, the exact etiology and pathophysiology have not yet been fully elucidated.

Nowadays, AAAs are clinically diagnosed by either computed tomography, ultrasound or magnetic resonance imaging (MRI), yet those modalities only deliver information on the aneurysm anatomy, size and form. It is generally accepted that AAA size correlates with the probability for rupture and related clinical events. However, a growing body of literature argues that the pathophysiology of AAA expansion is more multifaceted, with inflammation and degradation of the extracellular matrix (ECM) playing a pivotal role. Visualizing the complex nature of aneurysms requires the development of novel imaging modalities that facilitate more detailed depiction of AAAs.

Magnetic resonance elastography (MRE) is an imaging technology that combines low-frequency vibrations and MRI to create stiffness maps of body tissues. Remodeling of the ECM during AAA progression leads to stiffness changes, providing a potential imaging marker. Therefore, we assessed murine aneurysms by *ex vivo* microscopic multifrequency magnetic resonance elastography (μMMRE). By examining the aneurysmal thrombus, we discovered that regional variations in stiffness were strongly correlated to local histology-quantified ECM accumulation. With this proof-of-concept study, we demonstrated that MRE represents a suitable method for detecting shear wave speed changes reflected in varying stiffness values in the aneurysmal thrombus that in turn are representative of ECM remodeling. With successful clinical translation, this imaging modality could help detect potential fatal changes in the biomechanical structure of the AAA mimicked by ECM changes.

Magnetic particle imaging (MPI) is an innovative imaging modality, enabling a highly sensitive detection of magnetic nanoparticles (MNPs). Since MNPs are a suitable surrogate marker for molecular targeting of macrophages and the aneurysmal development involves inflammation as a fundamental process, we tested the feasibility of imaging AAA inflammation with MPI. We demonstrated that the MNP accumulation in *ex vivo* murine aneurysms can be visualized and quantified with MPI. In addition, the colocalization of macrophages and MNPs was visible in

histology. The ability to detect the spatial distribution and local concentration of MNPs establishes MPI as a promising tool for monitoring inflammatory progression in AAAs.

7 ZUSAMMENFASSUNG

Entwicklung und Evaluierung von neuartigen Bildgebungsmodalitäten für die Charakterisierung von abdominalen Aortenaneurysmen im Mausmodell

Als abdominales Aortenaneurysma (AAA) beschreibt man eine permanente, lokale Dilatation des abdominellen Anteils der Aorta, meist begleitet von einer Thrombusbildung. Eine Ruptur endet in über 90% der Fälle tödlich. Auch wenn AAAs heutzutage eine der häufigsten Ursachen für einen plötzlichen Tod darstellen, ist die genaue Ätiologie und Pathophysiologie bis heute nicht eindeutig entschlüsselt.

Die klinische Diagnose eines AAAs erfolgt heutzutage mittels Computertomographie, Ultraschall oder Magnetresonanztomographie (MRT), allerdings liefern die erwähnten Bildgebungsmodalitäten rein anatomische Informationen zu der Größe und Form des Aneurysmas. Im Allgemeinen wird angenommen, dass das Rupturrisiko mit der AAA Größe zusammenhängt. Mehrere Studien haben jedoch gezeigt, dass die Pathophysiologie der AAA Entwicklung facettenreich ist und dass Entzündung und Abbau der extrazellulären Matrix (EZM) eine zentrale Rolle spielen. Um die komplexe Natur des AAAs widerspiegeln zu können, benötigt man neuartige Bildgebungsmodalitäten, die einen detaillierten Einblick in die Biomechanik und Molekularbiologie ermöglichen.

Die Magnetresonanzelastographie (MRE) ist eine neuartige Bildgebungsmethode, die auf die kombinierte Anwendung von MRT und die Erzeugung von mechanischen Wellen für die viskoelastische Charakterisierung von Geweben beruht. Der Umbau der extrazellulären Matrix stellt ein zentrales Geschehen in der Pathophysiologie des AAA Fortschritts dar. Aus diesem Grund haben wir die Machbarkeit von MRE als bildgebendes Verfahren für die Analyse von *ex vivo* AAAs von Mäusen untersucht. Durch den Einsatz von MRE für die Bildgebung von dem AAA Thrombus konnten wir regionale Unterschiede in der Wellengeschwindigkeit nachweisen, was wiederum für regional unterschiedliche Gewebesteifigkeit spricht. Diese Unterschiede korrelierten stark mit der lokalen Verteilung und Konzentration von extrazellulären Matrixproteinen. Eine zukünftige klinische Translation dieser Methode würde zu einer verbesserten Einschätzung der biomechanischen Eigenschaften des AAAs führen, welches eine verbesserte Risikoeinschätzung ermöglicht.

Die Magnetpartikelbildgebung (MPI) stellt ebenso eine neuartige Bildgebungsmodalität dar. Dabei handelt es sich um die hochsensitive Detektion von magnetischen Nanopartikeln (MNPs) im Gewebe. MNPs stellen ein geeigneter indirekter Entzündungsmarker dar, da sie von Makrophagen am Ort des Entzündungsgeschehens aufgenommen werden. In unserer Studie haben wir die Umsetzbarkeit von MPI für die Bildgebung der Inflammation getestet. Wir

konnten die MNP Akkumulation in den *ex vivo* AAA-Mausproben darstellen, sowie die Kolokalisation von MNPs mit Makrophagen in der Histologie. Aufgrund der hochquantitativen und örtlich aufgelösten Eisendarstellung gehört MPI zu den vielversprechendsten zukünftigen bildgebenden Verfahren für AAAs in der medizinischen Diagnostik.

8 REFERENCES

Adolph, R., D. A. Vorp, D. L. Steed, M. W. Webster, M. V. Kameneva and S. C. Watkins (1997). "Cellular content and permeability of intraluminal thrombus in abdominal aortic aneurysm." Journal of Vascular Surgery 25(5): 916-926.

Alcorn, H. G., S. K. Wolfson, Jr., K. Sutton-Tyrrell, L. H. Kuller and D. O'Leary (1996). "Risk factors for abdominal aortic aneurysms in older adults enrolled in The Cardiovascular Health Study." Arterioscler Thromb Vasc Biol 16(8): 963-970.

Allaire, E., B. Muscatelli-Groux, C. Mandet, A. M. Guinault, P. Bruneval, P. Desgranges, A. Clowes, D. Melliere and J. P. Becquemin (2002). "Paracrine effect of vascular smooth muscle cells in the prevention of aortic aneurysm formation." J Vasc Surg 36(5): 1018-1026.

Bailey, A. (2001). "Molecular mechanisms of ageing in connective tissues." Mechanisms of Ageing and Development 122(7): 735-755.

Bakenecker, A. C., M. Ahlborg, C. Debbeler, C. Kaethner, T. M. Buzug and K. Ludtke-Buzug (2018). "Magnetic particle imaging in vascular medicine." Innov Surg Sci 3(3): 179-192.

Barrett, H. E., E. M. Cunnane, H. Hidayat, J. M. O'Brien, M. A. Moloney, E. G. Kavanagh and M. T. Walsh (2018). "On the influence of wall calcification and intraluminal thrombus on prediction of abdominal aortic aneurysm rupture." J Vasc Surg 67(4): 1234-1246 e1232.

Bergoeing, M. P., B. Arif, A. E. Hackmann, T. L. Ennis, R. W. Thompson and J. A. Curci (2007). "Cigarette smoking increases aortic dilatation without affecting matrix metalloproteinase-9 and -12 expression in a modified mouse model of aneurysm formation." J Vasc Surg 45(6): 1217-1227.

Bertalan, G., J. Guo, H. Tzschatzsch, C. Klein, E. Barnhill, I. Sack and J. Braun (2019). "Fast tomoelastography of the mouse brain by multifrequency single-shot MR elastography." Magn Reson Med 81(4): 2676-2687.

Bhamidipati, C. M., G. S. Mehta, G. Lu, C. W. Moehle, C. Barbery, P. D. DiMusto, A. Laser, I. L. Kron, G. R. Upchurch, Jr. and G. Ailawadi (2012). "Development of a novel murine model of aortic aneurysms using peri-adventitial elastase." Surgery 152(2): 238-246.

Bi, Y., H. Zhong, K. Xu, Y. Ni, X. Qi, Z. Zhang and W. Li (2013). "Performance of a modified rabbit model of abdominal aortic aneurysm induced by topical application of porcine elastase: 5-month follow-up study." Eur J Vasc Endovasc Surg 45(2): 145-152.

Bi, Y., H. Zhong, K. Xu, X. Qi, Z. Zhang, G. Wu and X. Han (2015). "Novel experimental model of enlarging abdominal aortic aneurysm in rabbits." J Vasc Surg 62(4): 1054-1063.

Bi, Y., H. Zhong, K. Xu, Z. Zhang, X. Qi, Y. Xia and L. Ren (2013). "Development of a novel rabbit model of abdominal aortic aneurysm via a combination of periaortic calcium chloride and elastase incubation." PLoS One 8(7): e68476.

Biasetti, J., T. C. Gasser, M. Auer, U. Hedin and F. Labruto (2010). "Hemodynamics of the normal aorta compared to fusiform and saccular abdominal aortic aneurysms with emphasis on a potential thrombus formation mechanism." Ann Biomed Eng 38(2): 380-390.

Billings, C., M. Langley, G. Warrington, F. Mashali and J. A. Johnson (2021). "Magnetic Particle Imaging: Current and Future Applications, Magnetic Nanoparticle Synthesis Methods and Safety Measures." Int J Mol Sci 22(14).

Borgert, J., J. D. Schmidt, I. Schmale, C. Bontus, B. Gleich, B. David, J. Weizenecker, J. Jockram, C. Lauruschkat, O. Mende, M. Heinrich, A. Halkola, J. Bergmann, O. Woywode and J. Rahmer (2013). "Perspectives on clinical magnetic particle imaging." Biomed Tech (Berl) 58(6): 551-556.

Borhani, M., J. K. Lee, T. L. Ennis and R. W. Thompson (2000). "Enalapril suppresses experimental aortic aneurysm formation in mice: evidence for a novel molecular mechanism distinct from angiotensin converting enzyme (ACE) inhibition." Journal of the American College of Surgeons 191(4).

Boudghène, F., S. Anidjar, E. Allaire, M. Osborne-Pellegrin, J.-M. Bigot and J.-B. Michel (1993). "Endovascular Grafting in Elastase-induced Experimental Aortic Aneurysms in Dogs: Feasibility and Preliminary Results." Journal of Vascular and Interventional Radiology 4(4): 497-504.

Brangsch, J., C. Reimann, J. O. Kaufmann, L. C. Adams, D. C. Onthank, C. Thone-Reineke, S. P. Robinson, R. Buchholz, U. Karst, R. M. Botnar, B. Hamm and M. R. Makowski (2019). "Concurrent Molecular Magnetic Resonance Imaging of Inflammatory Activity and Extracellular Matrix Degradation for the Prediction of Aneurysm Rupture." Circ Cardiovasc Imaging 12(3): e008707.

Broome, D. R. (2008). "Nephrogenic systemic fibrosis associated with gadolinium based contrast agents: a summary of the medical literature reporting." Eur J Radiol 66(2): 230-234.

Brophy, C., J. E. Tilson and M. D. Tilson (1988). "Propranolol delays the formation of aneurysms in the male blotchy mouse." J Surg Res 44(6): 687-689.

Brophy, C. M., J. E. Tilson, I. M. Braverman and M. D. Tilson (1988). "Age of onset, pattern of distribution, and histology of aneurysm development in a genetically predisposed mouse model." Journal of Vascular Surgery 8(1): 45-48.

Buckley, C., C. W. Wyble, M. Borhani, T. L. Ennis, D. K. Kobayashi, J. A. Curci, S. D. Shapiro and R. W. Thompson (2004). "Accelerated enlargement of experimental abdominal aortic aneurysms in a mouse model of chronic cigarette smoke exposure." J Am Coll Surg 199(6): 896-903.

Bulte, J. W. and D. L. Kraitchman (2004). "Iron oxide MR contrast agents for molecular and cellular imaging." NMR Biomed 17(7): 484-499.

Bulte, J. W. M. (2019). "Superparamagnetic iron oxides as MPI tracers: A primer and review of early applications." Adv Drug Deliv Rev 138: 293-301.

Busch, A., S. Bleichert, N. Ibrahim, M. Wortmann, H. H. Eckstein, C. Brostjan, M. U. Wagenhauser, C. J. Goergen and L. Maegdefessel (2021). "Translating mouse models of abdominal aortic aneurysm to the translational needs of vascular surgery." JVS Vasc Sci 2: 219-234.

Buzug, T. M., G. Bringout, M. Erbe, K. Grafe, M. Graeser, M. Gruttner, A. Halkola, T. F. Sattel, W. Tenner, H. Wojtczyk, J. Haegele, F. M. Vogt, J. Barkhausen and K. Ludtke-Buzug (2012). "Magnetic particle imaging: introduction to imaging and hardware realization." Z Med Phys 22(4): 323-334.

Cantisani, V., H. Grazhdani, D. A. Clevert, R. Iezzi, L. Aiani, A. Martegani, F. Fanelli, L. Di Marzo, A. Wlderk, C. Cirelli, C. Catalano, N. Di Leo, M. Di Segni, F. Malpassini and F. D'Ambrosio (2015). "EVAR: Benefits of CEUS for monitoring stent-graft status." Eur J Radiol 84(9): 1658-1665.

Cassis, L. A., M. Gupte, S. Thayer, X. Zhang, R. Charnigo, D. A. Howatt, D. L. Rateri and A. Daugherty (2009). "ANG II infusion promotes abdominal aortic aneurysms independent of increased blood pressure in hypercholesterolemic mice." Am J Physiol Heart Circ Physiol 296(5): H1660-1665.

Chiou, A. C., B. Chiu and W. H. Pearce (2001). "Murine aortic aneurysm produced by periarterial application of calcium chloride." J Surg Res 99(2): 371-376.

Corriere, M. A. and R. J. Guzman (2005). "True and false aneurysms of the femoral artery." Semin Vasc Surg 18(4): 216-223.

Curci, J. A., S. Liao, M. D. Huffman, S. D. Shapiro and R. W. Thompson (1998). "Expression and localization of macrophage elastase (matrix metalloproteinase-12) in abdominal aortic aneurysms." J Clin Invest 102(11): 1900-1910.

Czerski A, B. J., Gnus J, Hauzer W, Ratajczak K, Nowak M, Janeczek M, Zawadzki W, Witkiewicz W, Rusiecka A (2013). "Experimental methods of abdominal aortic aneurysm creation in swine as a large animal model." J Physiol Pharmacol.

Dai, J., L. Louedec, M. Philippe, J. B. Michel and X. Houard (2009). "Effect of blocking platelet activation with AZD6140 on development of abdominal aortic aneurysm in a rat aneurysmal model." J Vasc Surg 49(3): 719-727.

Dale, M. A., M. K. Ruhlman and B. T. Baxter (2015). "Inflammatory cell phenotypes in AAAs: their role and potential as targets for therapy." Arterioscler Thromb Vasc Biol 35(8): 1746-1755.

Daugherty, A. and L. A. Cassis (2002). "Mechanisms of abdominal aortic aneurysm formation." Curr Atheroscler Rep 4(3): 222-227.

Daugherty, A., M. W. Manning and L. A. Cassis (2000). "Angiotensin II promotes atherosclerotic lesions and aneurysms in apolipoprotein E-deficient mice." J Clin Invest 105(11): 1605-1612.

Daugherty, A., D. L. Rateri and L. A. Cassis (2006). "Role of the renin-angiotensin system in the development of abdominal aortic aneurysms in animals and humans." Ann N Y Acad Sci 1085: 82-91.

Davies, M. J. (1998). "Aortic aneurysm formation: lessons from human studies and experimental models." Circulation 98(3): 193-195.

Di Ieva, A., F. Grizzi, E. Rognone, Z. T. Tse, T. Parittotokkaporn, Y. B. F. Rodriguez, M. Tschabitscher, C. Matula, S. Trattnig and Y. B. R. Rodriguez (2010). "Magnetic resonance elastography: a general overview of its current and future applications in brain imaging." Neurosurg Rev 33(2): 137-145; discussion 145.

Di Martino, E., S. Mantero, F. Inzoli, G. Melissano, D. Astore, R. Chiesa and R. Fumero (1998). "Biomechanics of abdominal aortic aneurysm in the presence of endoluminal thrombus: Experimental characterisation and structural static computational analysis." European Journal of Vascular and Endovascular Surgery 15(4): 290-299.

Diez, J. (2007). "Arterial stiffness and extracellular matrix." Adv Cardiol 44: 76-95.

Dobrin, P. B. and R. Mrkvicka (1994). "Failure of Elastin or Collagen as Possible Critical Connective Tissue Alterations Underlying Aneurysmal Dilatation." Cardiovascular Surgery 2(4): 484-488.

Dobrovolskaia, M. A., M. Shurin and A. A. Shvedova (2016). "Current understanding of interactions between nanoparticles and the immune system." Toxicol Appl Pharmacol 299: 78-89.

Dong, H., R. Mazumder, V. S. P. Illapani, X. Mo, R. D. White and A. Kolipaka (2017). "In vivo quantification of aortic stiffness using MR elastography in hypertensive porcine model." Magn Reson Med 78(6): 2315-2321.

Dong, H., D. S. Russell, A. S. Litsky, M. E. Joseph, X. Mo, R. D. White and A. Kolipaka (2020). "In Vivo Aortic Magnetic Resonance Elastography in Abdominal Aortic Aneurysm: A Validation in an Animal Model." Invest Radiol 55(7): 463-472.

Dubost, C., M. Allary and N. Oeconomos (1951). "[Treatment of aortic aneurysms; removal of the aneurysm; re-establishment of continuity by grafts of preserved human aorta]." Mem Acad Chir (Paris) 77(12-13): 381-383.

Eiseman, B. and R. H. Hughes (1956). "Repair of an abdominal aortic vena caval fistula caused by rupture of an atherosclerotic aneurysm." Surgery 39(3): 498-504.

Elefteriades, J. A. and E. A. Farkas (2010). "Thoracic aortic aneurysm clinically pertinent controversies and uncertainties." J Am Coll Cardiol 55(9): 841-857.

Eliason, J. L., K. K. Hannawa, G. Ailawadi, I. Sinha, J. W. Ford, M. P. Deogracias, K. J. Roelofs, D. T. Woodrum, T. L. Ennis, P. K. Henke, J. C. Stanley, R. W. Thompson and G. R. Upchurch, Jr. (2005). "Neutrophil depletion inhibits experimental abdominal aortic aneurysm formation." Circulation 112(2): 232-240.

Erentug, V., N. Bozbuga, S. N. Omeroglu, H. Ardal, E. Eren, M. Guclu, F. Guzelmeric, K. Kirali, E. Akinci and C. Yakut (2003). "Rupture of abdominal aortic aneurysms in Behcet's disease." Ann Vasc Surg 17(6): 682-685.

Eskandari, M. K., J. D. Vijungco, A. Flores, J. Borensztajn, V. Shively and W. H. Pearce (2005). "Enhanced abdominal aortic aneurysm in TIMP-1-deficient mice." J Surg Res 123(2): 289-293.

Folkesson, M., N. Sadowska, S. Vikingsson, M. Karlsson, C. J. Carlhall, T. Lanne, D. Wagsater and L. Jensen (2016). "Differences in cardiovascular toxicities associated with cigarette smoking and snuff use revealed using novel zebrafish models." Biol Open 5(7): 970-978.

Fontaine, V., M.-P. Jacob, X. Houard, P. Rossignol, D. Plissonnier, E. Angles-Cano and J.-B. Michel (2002). "Involvement of the Mural Thrombus as a Site of Protease Release and Activation in Human Aortic Aneurysms." The American Journal of Pathology 161(5): 1701-1710.

Franke, J., U. Heinen, H. Lehr, A. Weber, F. Jaspard, W. Ruhm, M. Heidenreich and V. Schulz (2016). "System Characterization of a Highly Integrated Preclinical Hybrid MPI-MRI Scanner." IEEE Trans Med Imaging 35(9): 1993-2004.

Franke, J., U. Heinen, L. Matthies, V. Niemann, F. Jaspard, M. Heidenreich and T. M. Buzug (2013). "First hybrid MPI-MRI imaging system as integrated design for mice and rats: Description of the instrumentation setup." IWMPI.

Furusho, A., H. Aoki, S. Ohno-Urabe, M. Nishihara, S. Hirakata, N. Nishida, S. Ito, M. Hayashi, T. Imaizumi, S. Hiromatsu, H. Akashi, H. Tanaka and Y. Fukumoto (2018). "Involvement of B Cells, Immunoglobulins, and Syk in the Pathogenesis of Abdominal Aortic Aneurysm." J Am Heart Assoc 7(6).

Galle, C., L. Schandene, P. Stordeur, Y. Peignois, J. Ferreira, J. C. Wautrecht, J. P. Dereume and M. Goldman (2005). "Predominance of type 1 CD4+ T cells in human abdominal aortic aneurysm." Clin Exp Immunol 142(3): 519-527.

Gandhi, R. H., E. Irizarry, J. O. Cantor, S. Keller, G. B. Nackman, V. J. Halpern, K. M. Newman and M. D. Tilson (1994). "Analysis of elastin cross-linking and the connective tissue matrix of abdominal aortic aneurysms." Surgery 115(5): 617-620.

GBD 2013 Mortality and Causes of Death Collaborators (2015). "Global, regional, and national age–sex specific all-cause and cause-specific mortality for 240 causes of death, 1990–2013: a systematic analysis for the Global Burden of Disease Study 2013." The Lancet 385(9963): 117-171.

Geppert, M. and M. Himly (2021). "Iron Oxide Nanoparticles in Bioimaging - An Immune Perspective." Front Immunol 12: 688927.

Gleich, B. (2013). Principles and Applications of Magnetic Particle Imaging. Wiesbaden, Germany, Springer Vieweg.

Gleich, B. and J. Weizenecker (2005). "Tomographic imaging using the nonlinear response of magnetic particles." Nature 435(7046): 1214-1217.

Goergen, C. J., J. Azuma, K. N. Barr, L. Magdefessel, D. Y. Kallop, A. Gogineni, A. Grewall, R. M. Weimer, A. J. Connolly, R. L. Dalman, C. A. Taylor, P. S. Tsao and J. M. Greve (2011). "Influences of aortic motion and curvature on vessel expansion in murine experimental aneurysms." Arterioscler Thromb Vasc Biol 31(2): 270-279.

Goldfarb, S., P. A. McCullough, J. McDermott and S. B. Gay (2009). "Contrast-induced acute kidney injury: specialty-specific protocols for interventional radiology, diagnostic computed tomography radiology, and interventional cardiology." Mayo Clin Proc 84(2): 170-179.

Golledge, A. L., P. Walker, P. E. Norman and J. Golledge (2009). "A systematic review of studies examining inflammation associated cytokines in human abdominal aortic aneurysm samples." Dis Markers 26(4): 181-188.

Golledge, J. (2019). "Abdominal aortic aneurysm: update on pathogenesis and medical treatments." Nat Rev Cardiol 16(4): 225-242.

Golledge, J., J. Muller, A. Daugherty and P. Norman (2006). "Abdominal aortic aneurysm: pathogenesis and implications for management." Arterioscler Thromb Vasc Biol 26(12): 2605-2613.

Golledge, J. and P. E. Norman (2010). "Atherosclerosis and abdominal aortic aneurysm: cause, response, or common risk factors?" Arterioscler Thromb Vasc Biol 30(6): 1075-1077.

Goodwill, P. W., A. Tamrazian, L. R. Croft, C. D. Lu, L. M. Johnson, R. Pidaparthi, R. M. Ferguson, R. P. Khandhar, K. M.-. Krishnan and S. M. Conolly (2011). "Ferrohydrodynamic relaxometry for magnetic particle imaging." Appl. Phys. Lett. 98.

Haegele, J., J. Rahmer, B. Gleich, J. Borgert, H. Wojtczyk, N. Panagiotopoulos, T. M. Buzug, J. Barkhausen and F. M. Vogt (2012). "Magnetic particle imaging: visualization of instruments for cardiovascular intervention." Radiology 265(3): 933-938.

Haller, S. J., J. D. Crawford, K. M. Courchaine, C. J. Bohannan, G. J. Landry, G. L. Moneta, A. F. Azarbal and S. Rugonyi (2018). "Intraluminal thrombus is associated with early rupture of abdominal aortic aneurysm." J Vasc Surg 67(4): 1051-1058 e1051.

Halloran, B. G., V. A. Davis, B. M. McManus, T. G. Lynch and B. T. Baxter (1995). "Localization of aortic disease is associated with intrinsic differences in aortic structure." J Surg Res 59(1): 17-22.

Hance, K. A., M. Tataria, S. J. Ziporin, J. K. Lee and R. W. Thompson (2002). "Monocyte chemotactic activity in human abdominal aortic aneurysms: role of elastin degradation peptides and the 67-kD cell surface elastin receptor." J Vasc Surg 35(2): 254-261.

Harkness, M. L., R. D. Harkness and D. D. Mc (1955). "The collagen and elastin content of the arterial wall." J Physiol 127(2): 33-34P.

Hellenthal, F. A., W. A. Buurman, W. K. Wodzig and G. W. Schurink (2009). "Biomarkers of AAA progression. Part 1: extracellular matrix degeneration." Nat Rev Cardiol 6(7): 464-474.

Henke, P. K., J. D. Cardneau, T. H. Welling, 3rd, G. R. Upchurch, Jr., T. W. Wakefield, L. A. Jacobs, S. B. Proctor, L. J. Greenfield and J. C. Stanley (2001). "Renal artery aneurysms: a 35-year clinical experience with 252 aneurysms in 168 patients." Ann Surg 234(4): 454-462; discussion 462-453.

Henriques, T. A., J. Huang, S. S. D'Souza, A. Daugherty and L. A. Cassis (2004). "Orchidectomy, but not ovariectomy, regulates angiotensin II-induced vascular diseases in apolipoprotein E-deficient mice." Endocrinology 145(8): 3866-3872.

Hirsch, S., J. Braun and I. Sack (2017). Magnetic Resonance Elastography: Physical Background and Medical Applications, Wiley-VCH Verlag GmbH & Co. KGaA.

Hong, H., Y. Yang, B. Liu and W. Cai (2010). "Imaging of Abdominal Aortic Aneurysm: the present and the future." Curr Vasc Pharmacol 8(6): 808-819.

Hoodeshenas, S., M. Yin and S. K. Venkatesh (2018). "Magnetic Resonance Elastography of Liver: Current Update." Top Magn Reson Imaging 27(5): 319-333.

Hynecek, R. L., B. G. DeRubertis, S. M. Trocciola, H. Zhang, M. R. Prince, T. L. Ennis, K. C. Kent and P. L. Faries (2007). "The creation of an infrarenal aneurysm within the native abdominal aorta of swine." Surgery 142(2): 143-149.

Itoga, N. K., K. A. Rothenberg, P. Suarez, T. V. Ho, M. W. Mell, B. Xu, C. M. Curtin and R. L. Dalman (2019). "Metformin prescription status and abdominal aortic aneurysm disease progression in the U.S. veteran population." J Vasc Surg 69(3): 710-716 e713.

Jacomelli, J., L. Summers, A. Stevenson, T. Lees and J. J. Earnshaw (2017). "Editor's Choice - Inequalities in Abdominal Aortic Aneurysm Screening in England: Effects of Social Deprivation and Ethnicity." Eur J Vasc Endovasc Surg 53(6): 837-843.

Jahangir, E., L. Lipworth, T. L. Edwards, E. K. Kabagambe, M. T. Mumma, G. A. Mensah, S. Fazio, W. J. Blot and U. K. Sampson (2015). "Smoking, sex, risk factors and abdominal aortic aneurysms: a prospective study of 18 782 persons aged above 65 years in the Southern Community Cohort Study." J Epidemiol Community Health 69(5): 481-488.

Jamrozik, K., P. E. Norman, C. A. Spencer, R. W. Parsons, R. Tuohy, M. M. Lawrence-Brown and J. A. Dickinson (2000). "Screening for abdominal aortic aneurysm: lessons from a population-based study." Med J Aust 173(7): 345-350.

Ji, K., Y. Zhang, F. Jiang, L. Qian, H. Guo, J. Hu, L. Liao and J. Tang (2014). "Exploration of the mechanisms by which 3,4-benzopyrene promotes angiotensin II-induced abdominal aortic aneurysm formation in mice." J Vasc Surg 59(2): 492-499.

Jiang, F., G. T. Jones and G. J. Dusting (2007). "Failure of antioxidants to protect against angiotensin II-induced aortic rupture in aged apolipoprotein(E)-deficient mice." Br J Pharmacol 152(6): 880-890.

Jones, G. T., G. Tromp, H. Kuivaniemi, S. Gretarsdottir, A. F. Baas, B. Giusti, E. Strauss, F. N. Van't Hof, T. R. Webb, R. Erdman, M. D. Ritchie, J. R. Elmore, A. Verma, S. Pendergrass, I. J. Kullo, Z. Ye, P. L. Peissig, O. Gottesman, S. S. Verma, J. Malinowski, L. J. Rasmussen-Torvik, K. M. Borthwick, D. T. Smelser, D. R. Crosslin, M. de Andrade, E. J. Ryer, C. A. McCarty, E. P. Bottinger, J. A. Pacheco, D. C. Crawford, D. S. Carrell, G. S. Gerhard, D. P. Franklin, D. J. Carey, V. L. Phillips, M. J. Williams, W. Wei, R. Blair, A. A. Hill, T. M. Vasudevan, D. R. Lewis, I. A. Thomson, J. Krysa, G. B. Hill, J. Roake, T. R. Merriman, G. Oszkinis, S. Galora, C. Saracini, R. Abbate, R. Pulli, C. Pratesi, A. Saratzis, A. R. Verissimo, S. Bumpstead, S. A. Badger, R. E. Clough, G. Cockerill, H. Hafez, D. J. Scott, T. S. Futers, S. P. Romaine, K. Bridge, K. J. Griffin, M. A. Bailey, A. Smith, M. M. Thompson, F. M. van Bockxmeer, S. E. Matthiasson, G. Thorleifsson, U. Thorsteinsdottir, J. D. Blankensteijn, J. A. Teijink, C. Wijmenga, J. de Graaf, L. A. Kiemeney, J. S. Lindholt, A. Hughes, D. T. Bradley, K. Stirrups, J. Golledge, P. E. Norman, J. T. Powell, S. E. Humphries, S. E. Hamby, A. H. Goodall, C. P. Nelson, N. Sakalihasan, A. Courtois, R. E. Ferrell, P. Eriksson, L. Folkersen, A. Franco-Cereceda, J. D. Eicher, A. D. Johnson, C. Betsholtz, A. Ruusalepp, O. Franzen, E. E. Schadt, J. L. Bjorkegren, L. Lipovich, A. M. Drolet, E. L. Verhoeven, C. J. Zeebregts, R. H. Geelkerken, M. R. van Sambeek, S. M. van Sterkenburg, J. P. de Vries, K. Stefansson, J. R. Thompson, P. I. de Bakker, P. Deloukas, R. D. Sayers, S. C. Harrison, A. M. van Rij, N. J. Samani and M. J. Bown (2017). "Meta-Analysis of Genome-Wide Association Studies for Abdominal Aortic Aneurysm Identifies Four New Disease-Specific Risk Loci." Circ Res 120(2): 341-353.

Kalapatapu, V. R., K. R. Shelton, A. T. Ali, M. M. Moursi and J. F. Eidt (2008). "Pseudoaneurysm: a review." Curr Treat Options Cardiovasc Med 10(2): 173-183.

Kanematsu, Y., M. Kanematsu, C. Kurihara, T. L. Tsou, Y. Nuki, E. I. Liang, H. Makino and T. Hashimoto (2010). "Pharmacologically induced thoracic and abdominal aortic aneurysms in mice." Hypertension 55(5): 1267-1274.

Kaul, M. G., T. Mummert, C. Jung, J. Salamon, A. P. Khandhar, R. M. Ferguson, S. J. Kemp, H. Ittrich, K. M. Krishnan, G. Adam and T. Knopp (2017). "In vitro and in vivo comparison of a tailored magnetic particle imaging blood pool tracer with Resovist." Phys Med Biol 62(9): 3454-3469.

Kazi, M., J. Thyberg, P. Religa, J. Roy, P. Eriksson, U. Hedin and J. Swedenborg (2003). "Influence of intraluminal thrombus on structural and cellular composition of abdominal aortic aneurysm wall." Journal of Vascular Surgery 38(6): 1283-1292.

Keeling, W. B., P. A. Armstrong, P. A. Stone, D. F. Bandyk and M. L. Shames (2005). "An overview of matrix metalloproteinases in the pathogenesis and treatment of abdominal aortic aneurysms." Vasc Endovascular Surg 39(6): 457-464.

Kent, K. C. (2014). "Clinical practice. Abdominal aortic aneurysms." N Engl J Med 371(22): 2101-2108.

Khan, S., F. Fakhouri, W. Majeed and A. Kolipaka (2018). "Cardiovascular magnetic resonance elastography: A review." NMR Biomed 31(10): e3853.

Klink, A., J. Heynens, B. Herranz, M. E. Lobatto, T. Arias, H. M. Sanders, G. J. Strijkers, M. Merkx, K. Nicolay, V. Fuster, A. Tedgui, Z. Mallat, W. J. Mulder and Z. A. Fayad (2011). "In vivo characterization of a new abdominal aortic aneurysm mouse model with conventional and molecular magnetic resonance imaging." J Am Coll Cardiol 58(24): 2522-2530.

Knopp, T., N. Gdaniec and M. Moddel (2017). "Magnetic particle imaging: from proof of principle to preclinical applications." Phys Med Biol 62(14): R124-R178.

Koch, A. E., G. K. Haines, R. J. Rizzo, J. A. Radosevich, R. M. Pope, P. G. Robinson and W. H. Pearce (1990). "Human abdominal aortic aneurysms. Immunophenotypic analysis suggesting an immune-mediated response." Am J Pathol 137(5): 1199-1213.

Koch, A. E., S. L. Kunkel, W. H. Pearce, M. R. Shah, D. Parikh, H. L. Evanoff, G. K. Haines, M. D. Burdick and R. M. Strieter (1993). "Enhanced production of the chemotactic cytokines interleukin-8 and monocyte chemoattractant protein-1 in human abdominal aortic aneurysms." Am J Pathol 142(5): 1423-1431.

Kokje, V. B., J. F. Hamming and J. H. Lindeman (2015). "Editor's Choice - Pharmaceutical Management of Small Abdominal Aortic Aneurysms: A Systematic Review of the Clinical Evidence." Eur J Vasc Endovasc Surg 50(6): 702-713.

Kolipaka, A., V. S. Illapani, W. Kenyhercz, J. D. Dowell, M. R. Go, J. E. Starr, P. S. Vaccaro and R. D. White (2016). "Quantification of abdominal aortic aneurysm stiffness using magnetic resonance elastography and its comparison to aneurysm diameter." J Vasc Surg 64(4): 966-974.

Kolipaka, A., D. Woodrum, P. A. Araoz and R. L. Ehman (2012). "MR elastography of the in vivo abdominal aorta: a feasibility study for comparing aortic stiffness between hypertensives and normotensives." J Magn Reson Imaging 35(3): 582-586.

Konova, E., S. Baydanoff, M. Atanasova and A. Velkova (2004). "Age-related changes in the glycation of human aortic elastin." Exp Gerontol 39(2): 249-254.

Kratz, H., A. Mohtashamdolatshahi, D. Eberbeck, O. Kosch, R. Hauptmann, F. Wiekhorst, M. Taupitz, B. Hamm and J. Schnorr (2019). "MPI Phantom Study with A High-Performing Multicore Tracer Made by Coprecipitation." Nanomaterials (Basel) 9(10).

Kratz, H., M. Taupitz, A. Ariza de Schellenberger, O. Kosch, D. Eberbeck, S. Wagner, L. Trahms, B. Hamm and J. Schnorr (2018). "Novel magnetic multicore nanoparticles designed for MPI and other biomedical applications: From synthesis to first in vivo studies." PLoS One 13(1): e0190214.

Krettek, A., G. K. Sukhova and P. Libby (2003). "Elastogenesis in human arterial disease: a role for macrophages in disordered elastin synthesis." Arterioscler Thromb Vasc Biol 23(4): 582-587.

Kuhlencordt, P. J., R. Gyurko, F. Han, M. Scherrer-Crosbie, T. H. Aretz, R. Hajjar, M. H. Picard and P. L. Huang (2001). "Accelerated atherosclerosis, aortic aneurysm formation, and ischemic heart disease in apolipoprotein E/endothelial nitric oxide synthase double-knockout mice." Circulation 104(4): 448-454.

Labruto, F., L. Blomqvist and J. Swedenborg (2011). "Imaging the intraluminal thrombus of abdominal aortic aneurysms: techniques, findings, and clinical implications." J Vasc Interv Radiol 22(8): 1069-1075; quiz 1075.

Larsson, E., F. Granath, J. Swedenborg and R. Hultgren (2009). "A population-based case-control study of the familial risk of abdominal aortic aneurysm." J Vasc Surg 49(1): 47-50; discussion 51.

Laser, A., G. Lu, A. Ghosh, K. Roelofs, B. McEvoy, P. DiMusto, C. M. Bhamidipati, G. Su, Y. Zhao, C. L. Lau, G. Ailawadi, J. L. Eliason, P. K. Henke and G. R. Upchurch, Jr. (2012). "Differential gender- and species-specific formation of aneurysms using a novel method of inducing abdominal aortic aneurysms." J Surg Res 178(2): 1038-1045.

Lawton, M. T., A. Quinones-Hinojosa, E. F. Chang and T. Yu (2005). "Thrombotic intracranial aneurysms: classification scheme and management strategies in 68 patients." Neurosurgery 56(3): 441-454; discussion 441-454.

Leach, J., E. Kao, C. Zhu, D. Saloner and M. D. Hope (2019). "On the relative impact of intraluminal thrombus heterogeneity on abdominal aortic aneurysm mechanics." J Biomech Eng.

Lederle, F. A. (2011). "The rise and fall of abdominal aortic aneurysm." Circulation 124(10): 1097-1099.

Lederle, F. A., G. R. Johnson, S. E. Wilson, D. J. Ballard, W. D. Jordan, Jr., J. Blebea, F. N. Littooy, J. A. Freischlag, D. Bandyk, J. H. Rapp, A. A. Salam and I. Veterans Affairs Cooperative Study (2002). "Rupture rate of large abdominal aortic aneurysms in patients refusing or unfit for elective repair." JAMA 287(22): 2968-2972.

Lederle, F. A., G. R. Johnson, S. E. Wilson, E. P. Chute, F. N. Littooy, D. Bandyk, W. C. Krupski, G. W. Barone, C. W. Acher and D. J. Ballard (1997). "Prevalence and associations of abdominal aortic aneurysm detected through screening. Aneurysm Detection and Management (ADAM) Veterans Affairs Cooperative Study Group." Ann Intern Med 126(6): 441-449.

Lee, A. T. and A. Cerami (1992). "Role of glycation in aging." Ann N Y Acad Sci 663: 63-70.

Lin, P. Y., Y. T. Wu, G. C. Lin, Y. H. Shih, A. Sampilvanjil, L. R. Chen, Y. J. Yang, H. L. Wu and M. J. Jiang (2013). "Coarctation-induced degenerative abdominal aortic aneurysm in a porcine model." J Vasc Surg 57(3): 806-815 e801.

Lindeman, J. H. N., H. Abdul-Hussien, J. H. van Bockel, R. Wolterbeek and R. Kleemann (2009). "Clinical Trial of Doxycycline for Matrix Metalloproteinase-9 Inhibition in Patients With an Abdominal Aneurysm." Circulation 119(16): 2209-2216.

Liu, S., A. Chiu-Lam, A. Rivera-Rodriguez, R. DeGroff, S. Savliwala, N. Sarna and C. M. Rinaldi-Ramos (2021). "Long circulating tracer tailored for magnetic particle imaging." Nanotheranostics 5(3): 348-361.

Lopez-Candales, A., D. R. Holmes, S. Liao, M. J. Scott, S. A. Wickline and R. W. Thompson (1997). "Decreased vascular smooth muscle cell density in medial degeneration of human abdominal aortic aneurysms." Am J Pathol 150(3): 993-1007.

Low, G., S. A. Kruse and D. J. Lomas (2016). "General review of magnetic resonance elastography." World J Radiol 8(1): 59-72.

Lu, G., G. Su, J. P. Davis, B. Schaheen, E. Downs, R. J. Roy, G. Ailawadi and G. R. Upchurch, Jr. (2017). "A novel chronic advanced stage abdominal aortic aneurysm murine model." J Vasc Surg 66(1): 232-242 e234.

Lu, H., D. A. Howatt, A. Balakrishnan, J. J. Moorleghen, D. L. Rateri, L. A. Cassis and A. Daugherty (2015). "Subcutaneous Angiotensin II Infusion using Osmotic Pumps Induces Aortic Aneurysms in Mice." J Vis Exp(103).

Lu, M., M. H. Cohen, D. Rieves and R. Pazdur (2010). "FDA report: Ferumoxytol for intravenous iron therapy in adult patients with chronic kidney disease." Am J Hematol 85(5): 315-319.

Lukasiewicz, A., J. Reszec, R. Kowalewski, L. Chyczewski and U. Lebkowska (2012). "Assessment of inflammatory infiltration and angiogenesis in the thrombus and the wall of abdominal aortic aneurysms on the basis of histological parameters and computed tomography angiography study." Folia Histochem Cytobiol 50(4): 547-553.

MA3RS Study Investigators (2017). "Aortic Wall Inflammation Predicts Abdominal Aortic Aneurysm Expansion, Rupture, and Need for Surgical Repair." Circulation 136(9): 787-797.

Maegdefessel, L., J. Azuma, R. Toh, A. Deng, D. R. Merk, A. Raiesdana, N. J. Leeper, U. Raaz, A. M. Schoelmerich, M. V. McConnell, R. L. Dalman, J. M. Spin and P. S. Tsao (2012).

"MicroRNA-21 blocks abdominal aortic aneurysm development and nicotine-augmented expansion." Sci Transl Med 4(122): 122ra122.

Maegdefessel, L., J. Azuma, R. Toh, D. R. Merk, A. Deng, J. T. Chin, U. Raaz, A. M. Schoelmerich, A. Raiesdana, N. J. Leeper, M. V. McConnell, R. L. Dalman, J. M. Spin and P. S. Tsao (2012). "Inhibition of microRNA-29b reduces murine abdominal aortic aneurysm development." J Clin Invest 122(2): 497-506.

Maegdefessel, L., J. M. Spin, U. Raaz, S. M. Eken, R. Toh, J. Azuma, M. Adam, F. Nakagami, H. M. Heymann, E. Chernogubova, H. Jin, J. Roy, R. Hultgren, K. Caidahl, S. Schrepfer, A. Hamsten, P. Eriksson, M. V. McConnell, R. L. Dalman and P. S. Tsao (2014). "miR-24 limits aortic vascular inflammation and murine abdominal aneurysm development." Nat Commun 5: 5214.

Makela, A. V., J. M. Gaudet, D. H. Murrell, J. R. Mansfield, M. Wintermark and C. H. Contag (2021). "Mind Over Magnets - How Magnetic Particle Imaging is Changing the Way We Think About the Future of Neuroscience." Neuroscience 474: 100-109.

Manduca, A., P. J. Bayly, R. L. Ehman, A. Kolipaka, T. J. Royston, I. Sack, R. Sinkus and B. E. Van Beers (2020). "MR elastography: Principles, guidelines, and terminology." Magn Reson Med.

Manduca, A., T. E. Oliphant, M. A. Dresner, J. L. Mahowald, S. A. Kruse, E. Amromin, J. P. Felmlee, J. F. Greenleaf and R. L. Ehman (2001). "Magnetic resonance elastography: non-invasive mapping of tissue elasticity." Med Image Anal 5(4): 237-254.

Manning, B. J., T. Kristmundsson, B. Sonesson and T. Resch (2009). "Abdominal aortic aneurysm diameter: a comparison of ultrasound measurements with those from standard and three-dimensional computed tomography reconstruction." J Vasc Surg 50(2): 263-268.

Manning, M. W., L. A. Cassis, J. Huang, S. J. Szilvassy and A. Daugherty (2002). "Abdominal aortic aneurysms: fresh insights from a novel animal model of the disease." Vasc Med 7(1): 45-54.

Mariappan, Y. K., K. J. Glaser and R. L. Ehman (2010). "Magnetic resonance elastography: a review." Clin Anat 23(5): 497-511.

Mata, K. M., P. S. Prudente, F. S. Rocha, C. M. Prado, E. M. Floriano, J. Elias, Jr., E. Rizzi, R. F. Gerlach, M. A. Rossi and S. G. Ramos (2011). "Combining two potential causes of metalloproteinase secretion causes abdominal aortic aneurysms in rats: a new experimental model." Int J Exp Pathol 92(1): 26-39.

Matsumura, K., T. Hirano, K. Takeda, A. Matsuda, T. Nakagawa, N. Yamaguchi, H. Yuasa, M. Kusakawa and T. Nakano (1991). "Incidence of aneurysms in Takayasu's arteritis." Angiology 42(4): 308-315.

McGee, G. S., B. T. Baxter, V. P. Shively, R. Chisholm, W. J. McCarthy, W. R. Flinn, J. S. Yao and W. H. Pearce (1991). "Aneurysm or occlusive disease--factors determining the clinical

course of atherosclerosis of the infrarenal aorta." Surgery 110(2): 370-375; discussion 375-376.

McGee, K. P., R. D. Hubmayr, D. Levin and R. L. Ehman (2009). "Feasibility of quantifying the mechanical properties of lung parenchyma in a small-animal model using (1)H magnetic resonance elastography (MRE)." J Magn Reson Imaging 29(4): 838-845.

McGrath, D. M., J. Lee, W. D. Foltz, N. Samavati, T. van der Kwast, M. A. Jewett, P. Chung, C. Menard and K. K. Brock (2017). "MR elastography to measure the effects of cancer and pathology fixation on prostate biomechanics, and comparison with T 1, T 2 and ADC." Phys Med Biol 62(3): 1126-1148.

Meijer, C. A. and T. Stigmen (2014). "Doxycycline for Stabilization of Abdominal Aortic Aneurysms: A Randomized Trial." Journal of Vascular Surgery 59(4): 1175-1176.

Menashi, S., J. S. Campa, R. M. Greenhalgh and J. T. Powell (1987). "Collagen in abdominal aortic aneurysm: Typing, content, and degradation." Journal of Vascular Surgery 6(6): 578-582.

Meng, X., J. Yang, K. Zhang, G. An, J. Kong, F. Jiang, Y. Zhang and C. Zhang (2014). "Regulatory T cells prevent angiotensin II-induced abdominal aortic aneurysm in apolipoprotein E knockout mice." Hypertension 64(4): 875-882.

Meola, A., J. Rao, N. Chaudhary, G. Song, X. Zheng and S. D. Chang (2019). "Magnetic Particle Imaging in Neurosurgery." World Neurosurg 125: 261-270.

Moher, D., C. W. Cole and G. B. Hill (1992). "Epidemiology of abdominal aortic aneurysm: The effect of differing definitions." European Journal of Vascular Surgery 6(6): 647-650.

Mohtashamdolatshahi, A., H. Kratz, O. Kosch, R. Hauptmann, N. Stolzenburg, F. Wiekhorst, I. Sack, B. Hamm, M. Taupitz and J. Schnorr (2020). "In vivo magnetic particle imaging: angiography of inferior vena cava and aorta in rats using newly developed multicore particles." Sci Rep 10(1): 17247.

Molacek, J., V. Treska, J. Kobr, B. Certik, T. Skalicky, V. Kuntscher and V. Krizkova (2009). "Optimization of the model of abdominal aortic aneurysm--experiment in an animal model." J Vasc Res 46(1): 1-5.

Moll, F. L., J. T. Powell, G. Fraedrich, F. Verzini, S. Haulon, M. Waltham, J. A. van Herwaarden, P. J. Holt, J. W. van Keulen, B. Rantner, F. J. Schlosser, F. Setacci, J. B. Ricco and S. European Society for Vascular (2011). "Management of abdominal aortic aneurysms clinical practice guidelines of the European society for vascular surgery." Eur J Vasc Endovasc Surg 41 Suppl 1: S1-S58.

Muthupillai, R. and R. L. Ehman (1996). "Magnetic resonance elastography." Nat Med 2(5): 601-603.

Nishijo, N., F. Sugiyama, K. Kimoto, K. Taniguchi, K. Murakami, S. Suzuki, A. Fukamizu and K. Yagami (1998). "Salt-sensitive aortic aneurysm and rupture in hypertensive transgenic mice that overproduce angiotensin II." Laboratory Investigation 78(9): 1059-1066.

Norman, P. E. and J. T. Powell (2007). "Abdominal Aortic Aneurysm: The prognosis in women is worse than in men " Circulation 115(22): 2865-2869.

Nyman, R. and M. O. Eriksson (2008). "The future of imaging in the management of abdominal aortic aneurysm." Scand J Surg 97(2): 110-115.

Ocana, E. (2003). "Characterisation of T and B lymphocytes infiltrating abdominal aortic aneurysms." Atherosclerosis 170(1): 39-48.

Ogata, Y., J. J. Enghild and H. Nagase (1992). "Matrix metalloproteinase 3 (stromelysin) activates the precursor for the human matrix metalloproteinase 9." Journal of Biological Chemistry 267(6): 3581-3584.

Oliver-Williams, C., M. J. Sweeting, G. Turton, D. Parkin, D. Cooper, C. Rodd, S. G. Thompson, J. J. Earnshaw, Gloucestershire and P. Swindon Abdominal Aortic Aneurysm Screening (2018). "Lessons learned about prevalence and growth rates of abdominal aortic aneurysms from a 25-year ultrasound population screening programme." Br J Surg 105(1): 68-74.

Panagiotopoulos, N., R. L. Duschka, M. Ahlborg, G. Bringout, C. Debbeler, M. Graeser, C. Kaethner, K. Ludtke-Buzug, H. Medimagh, J. Stelzner, T. M. Buzug, J. Barkhausen, F. M. Vogt and J. Haegele (2015). "Magnetic particle imaging: current developments and future directions." Int J Nanomedicine 10: 3097-3114.

Parkinson, F., S. Ferguson, P. Lewis, I. M. Williams, C. P. Twine and N. South East Wales Vascular (2015). "Rupture rates of untreated large abdominal aortic aneurysms in patients unfit for elective repair." J Vasc Surg 61(6): 1606-1612.

Parodi, J. C., J. C. Palmaz and H. D. Barone (1991). "Transfemoral intraluminal graft implantation for abdominal aortic aneurysms." Ann Vasc Surg 5(6): 491-499.

Patel, B. K., N. Samreen, Y. Zhou, J. Chen, K. Brandt, R. Ehman and K. Pepin (2021). "MR Elastography of the Breast: Evolution of Technique, Case Examples, and Future Directions." Clin Breast Cancer 21(1): e102-e111.

Patelis, N., D. Moris, D. Schizas, C. Damaskos, D. Perrea, C. Bakoyiannis, T. Liakakos and S. Georgopoulos (2017). "Animal models in the research of abdominal aortic aneurysms development." Physiol Res 66(6): 899-915.

Pearce, W. H., I. Sweis, J. S. Yao, W. J. McCarthy and A. E. Koch (1992). "Interleukin-1 beta and tumor necrosis factor-alpha release in normal and diseased human infrarenal aortas." J Vasc Surg 16(5): 784-789.

Pleumeekers, H. J., A. W. Hoes, E. van der Does, H. van Urk, A. Hofman, P. T. de Jong and D. E. Grobbee (1995). "Aneurysms of the abdominal aorta in older adults. The Rotterdam Study." Am J Epidemiol 142(12): 1291-1299.

Polzer, S., T. C. Gasser, J. Swedenborg and J. Bursa (2011). "The impact of intraluminal thrombus failure on the mechanical stress in the wall of abdominal aortic aneurysms." Eur J Vasc Endovasc Surg 41(4): 467-473.

Powell, J. T., M. J. Sweeting, P. Ulug, J. D. Blankensteijn, F. A. Lederle, J. P. Becquemin, R. M. Greenhalgh, D. O. Evar and A. C. E. Trialists (2017). "Meta-analysis of individual-patient data from EVAR-1, DREAM, OVER and ACE trials comparing outcomes of endovascular or open repair for abdominal aortic aneurysm over 5 years." Br J Surg 104(3): 166-178.

Pyo, R., J. K. Lee, J. M. Shipley, J. A. Curci, D. Mao, S. J. Ziporin, T. L. Ennis, S. D. Shapiro, R. M. Senior and R. W. Thompson (2000). "Targeted gene disruption of matrix metalloproteinase-9 (gelatinase B) suppresses development of experimental abdominal aortic aneurysms." J Clin Invest 105(11): 1641-1649.

Rahmer, J., J. Weizenecker, B. Gleich and J. Borgert (2009). "Signal encoding in magnetic particle imaging: properties of the system function." BMC Med Imaging 9: 4.

Rahmer, J., J. Weizenecker, B. Gleich and J. Borgert (2012). "Analysis of a 3-D system function measured for magnetic particle imaging." IEEE Trans Med Imaging 31(6): 1289-1299.

Riber, S. S., M. Ali, S. H. Bergseth, J. Stubbe, M. Stenger, C. Behr-Rasmussen and J. S. Lindholt (2017). "Induction of autoimmune abdominal aortic aneurysm in pigs - A novel large animal model." Ann Med Surg (Lond) 20: 26-31.

Ringleb, S. I., S. F. Bensamoun, Q. Chen, A. Manduca, K. N. An and R. L. Ehman (2007). "Applications of magnetic resonance elastography to healthy and pathologic skeletal muscle." J Magn Reson Imaging 25(2): 301-309.

Riveros, F., G. Martufi, T. C. Gasser and J. F. Rodriguez-Matas (2015). "On the Impact of Intraluminal Thrombus Mechanical Behavior in AAA Passive Mechanics." Ann Biomed Eng 43(9): 2253-2264.

Sack, I., B. Beierbach, J. Wuerfel, D. Klatt, U. Hamhaber, S. Papazoglou, P. Martus and J. Braun (2009). "The impact of aging and gender on brain viscoelasticity." Neuroimage 46(3): 652-657.

Sakalihasan, D., Nusgens, Limet, Lapière (1996). "Activated forms of MMP2 and MMP9 in abdominal aortic aneurysms." J. Vasc. Surg 24 127-133.

Sakalihasan, N., A. Heyeres, B. V. Nusgens, R. Limet and C. M. Lapiére (1993). "Modifications of the extracellular matrix of aneurysmal abdominal aortas as a function of their size." European Journal of Vascular Surgery 7(6): 633-637.

Sakalihasan, N., R. Limet and O. D. Defawe (2005). "Abdominal aortic aneurysm." The Lancet 365(9470): 1577-1589.

Sakalihasan, N., J. B. Michel, A. Katsargyris, H. Kuivaniemi, J. O. Defraigne, A. Nchimi, J. T. Powell, K. Yoshimura and R. Hultgren (2018). "Abdominal aortic aneurysms." Nat Rev Dis Primers 4(1): 34.

Sampson, U. K., P. E. Norman, F. G. Fowkes, V. Aboyans, S. Yanna, F. E. Harrell, Jr., M. H. Forouzanfar, M. Naghavi, J. O. Denenberg, M. M. McDermott, M. H. Criqui, G. A. Mensah, M. Ezzati and C. Murray (2014). "Global and regional burden of aortic dissection and aneurysms: mortality trends in 21 world regions, 1990 to 2010." Glob Heart 9(1): 171-180 e110.

Saraff, K., F. Babamusta, L. A. Cassis and A. Daugherty (2003). "Aortic dissection precedes formation of aneurysms and atherosclerosis in angiotensin II-infused, apolipoprotein E-deficient mice." Arterioscler Thromb Vasc Biol 23(9): 1621-1626.

Saritas, E. U., P. W. Goodwill, L. R. Croft, J. J. Konkle, K. Lu, B. Zheng and S. M. Conolly (2013). "Magnetic particle imaging (MPI) for NMR and MRI researchers." J Magn Reson 229: 116-126.

Sarvazyan, A. (1998). "Mechanical imaging: a new technology for medical diagnostics." Int J Med Inform 49(2): 195-216.

Satta, J., T. Juvonen, K. Haukipuro, M. Juvonen and M. I. Kairaluoma (1995). "Increased turnover of collagen in abdominal aortic aneurysms, demonstrated by measuring the concentration of the aminoterminal propeptide of type III procollagen in peripheral and aortal blood samples." J Vasc Surg 22(2): 155-160.

Schaafs, L. A., F. Schrank, C. Warmuth, I. G. Steffen, J. Braun, B. Hamm, I. Sack and T. Elgeti (2020). "Steady-State Multifrequency Magnetic Resonance Elastography of the Thoracic and Abdominal Human Aorta-Validation and Reference Values." Invest Radiol 55(7): 451-456.

Schneider, D. and K. Lüdtke-Buzug (2012). Biomaterials for regenerative medicine: Cytotoxicity of superparamagnetic iron oxide nanoparticles in stem cells. , Springer Proc Phys.: 117-122.

Schultz, G., M. M. Tedesco, E. Sho, T. Nishimura, S. Sharif, X. Du, T. Myles, J. Morser, R. L. Dalman and L. L. Leung (2010). "Enhanced abdominal aortic aneurysm formation in thrombin-activatable procarboxypeptidase B-deficient mice." Arterioscler Thromb Vasc Biol 30(7): 1363-1370.

Scott, R. A., L. G. Kim, H. A. Ashton and G. Multi-centre Aneurysm Screening Study (2005). "Assessment of the criteria for elective surgery in screen-detected abdominal aortic aneurysms." J Med Screen 12(3): 150-154.

Sedlacik, J., A. Frolich, J. Spallek, N. D. Forkert, T. D. Faizy, F. Werner, T. Knopp, D. Krause, J. Fiehler and J. H. Buhk (2016). "Magnetic Particle Imaging for High Temporal Resolution Assessment of Aneurysm Hemodynamics." PLoS One 11(8): e0160097.

Sehl, O. C. and P. J. Foster (2021). "The sensitivity of magnetic particle imaging and fluorine-19 magnetic resonance imaging for cell tracking." Sci Rep 11(1): 22198.

Shah, A. and M. A. Dobrovolskaia (2018). "Immunological effects of iron oxide nanoparticles and iron-based complex drug formulations: Therapeutic benefits, toxicity, mechanistic insights, and translational considerations." Nanomedicine 14(3): 977-990.

Sharma, A. K., G. Lu, A. Jester, W. F. Johnston, Y. Zhao, V. A. Hajzus, M. R. Saadatzadeh, G. Su, C. M. Bhamidipati, G. S. Mehta, I. L. Kron, V. E. Laubach, M. P. Murphy, G. Ailawadi and G. R. Upchurch, Jr. (2012). "Experimental abdominal aortic aneurysm formation is mediated by IL-17 and attenuated by mesenchymal stem cell treatment." Circulation 126(11 Suppl 1): S38-45.

Shire, N. J., M. Yin, J. Chen, R. A. Railkar, S. Fox-Bosetti, S. M. Johnson, C. R. Beals, B. J. Dardzinski, S. O. Sanderson, J. A. Talwalkar and R. L. Ehman (2011). "Test-retest repeatability of MR elastography for noninvasive liver fibrosis assessment in hepatitis C." J Magn Reson Imaging 34(4): 947-955.

Sillesen, H., N. Eldrup, R. Hultgren, J. Lindeman, K. Bredahl, M. Thompson, A. Wanhainen, U. Wingren, J. Swedenborg and A. T. Investigators (2015). "Randomized clinical trial of mast cell inhibition in patients with a medium-sized abdominal aortic aneurysm." Br J Surg 102(8): 894-901.

Singh, K., K. H. Bonaa, B. K. Jacobsen, L. Bjork and S. Solberg (2001). "Prevalence of and risk factors for abdominal aortic aneurysms in a population-based study : The Tromso Study." Am J Epidemiol 154(3): 236-244.

Singh, S., S. K. Venkatesh, A. Keaveny, S. Adam, F. H. Miller, P. Asbach, E. M. Godfrey, A. C. Silva, Z. Wang, M. H. Murad, S. K. Asrani, D. J. Lomas and R. L. Ehman (2016). "Diagnostic accuracy of magnetic resonance elastography in liver transplant recipients: A pooled analysis." Ann Hepatol 15(3): 363-376.

Steinmetz, E. F., C. Buckley, M. L. Shames, T. L. Ennis, S. J. Vanvickle-Chavez, D. Mao, L. A. Goeddel, C. J. Hawkins and R. W. Thompson (2005). "Treatment with simvastatin suppresses the development of experimental abdominal aortic aneurysms in normal and hypercholesterolemic mice." Ann Surg 241(1): 92-101.

Svensjo, S., M. Bjorck, M. Gurtelschmid, K. Djavani Gidlund, A. Hellberg and A. Wanhainen (2011). "Low prevalence of abdominal aortic aneurysm among 65-year-old Swedish men indicates a change in the epidemiology of the disease." Circulation 124(10): 1118-1123.

Szekanecz, Z., M. R. Shah, W. H. Pearce and A. E. Koch (1994). "Human atherosclerotic abdominal aortic aneurysms produce interleukin (IL)-6 and interferon-gamma but not IL-2 and IL-4: the possible role for IL-6 and interferon-gamma in vascular inflammation." Agents Actions 42(3-4): 159-162.

Takahashi, K., Y. Matsumoto, Z. Do e, M. Kanazawa, K. Satoh, T. Shimizu, A. Sato, Y. Fukumoto and H. Shimokawa (2013). "Combination therapy with atorvastatin and amlodipine suppresses angiotensin II-induced aortic aneurysm formation." PLoS One 8(8): e72558.

Tanaka, H., N. Zaima, T. Sasaki, M. Sano, N. Yamamoto, T. Saito, K. Inuzuka, T. Hayasaka, N. Goto-Inoue, Y. Sugiura, K. Sato, H. Kugo, T. Moriyama, H. Konno, M. Setou and N. Unno

(2015). "Hypoperfusion of the Adventitial Vasa Vasorum Develops an Abdominal Aortic Aneurysm." PLoS One 10(8): e0134386.

Tang, W., L. Yao, N. S. Roetker, A. Alonso, P. L. Lutsey, C. C. Steenson, F. A. Lederle, D. W. Hunter, L. G. Bengtson, W. Guan, E. Missov and A. R. Folsom (2016). "Lifetime Risk and Risk Factors for Abdominal Aortic Aneurysm in a 24-Year Prospective Study: The ARIC Study (Atherosclerosis Risk in Communities)." Arterioscler Thromb Vasc Biol 36(12): 2468-2477.

Tartaj, P., M. a. d. P. Morales, S. Veintemillas-Verdaguer, T. Gonz lez-Carre o and C. J. Serna (2003). "The preparation of magnetic nanoparticles for applications in biomedicine." Journal of Physics D: Applied Physics 36(13): R182-R197.

Tay, Z. W., P. Chandrasekharan, B. D. Fellows, I. R. Arrizabalaga, E. Yu, M. Olivo and S. M. Conolly (2021). "Magnetic Particle Imaging: An Emerging Modality with Prospects in Diagnosis, Targeting and Therapy of Cancer." Cancers (Basel) 13(21).

Temme, S., M. Yakoub, P. Bouvain, G. Yang, J. Schrader, J. Stegbauer and U. Flogel (2021). "Beyond Vessel Diameters: Non-invasive Monitoring of Flow Patterns and Immune Cell Recruitment in Murine Abdominal Aortic Disorders by Multiparametric MRI." Front Cardiovasc Med 8: 750251.

Thompson, A. R., J. A. Cooper, H. A. Ashton and H. Hafez (2010). "Growth rates of small abdominal aortic aneurysms correlate with clinical events." Br J Surg 97(1): 37-44.

Thompson, R. W., P. J. Geraghty and J. K. Lee (2002). "Abdominal aortic aneurysms: basic mechanisms and clinical implications." Curr Probl Surg 39(2): 110-230.

Thompson, S. G., H. A. Ashton, L. Gao, R. A. Scott and G. Multicentre Aneurysm Screening Study (2009). "Screening men for abdominal aortic aneurysm: 10 year mortality and cost effectiveness results from the randomised Multicentre Aneurysm Screening Study." BMJ 338: b2307.

Tomee, S. M., C. A. Meijer, D. A. Kies, S. le Cessie, M. Wasser, J. Golledge, J. F. Hamming and J. H. N. Lindeman (2021). "Systematic approach towards reliable estimation of abdominal aortic aneurysm size by ultrasound imaging and CT." BJS Open 5(1).

Tong, J., T. Cohnert, P. Regitnig and G. A. Holzapfel (2011). "Effects of age on the elastic properties of the intraluminal thrombus and the thrombus-covered wall in abdominal aortic aneurysms: biaxial extension behaviour and material modelling." Eur J Vasc Endovasc Surg 42(2): 207-219.

Townsley, M. M., I. Y. Soh and H. Ramakrishna (2021). "Endovascular Versus Open Aortic Reconstruction: A Comparison of Outcomes." J Cardiothorac Vasc Anesth 35(6): 1875-1883.

Trachet, B., L. Aslanidou, A. Piersigilli, R. A. Fraga-Silva, J. Sordet-Dessimoz, P. Villanueva-Perez, M. F. M. Stampanoni, N. Stergiopulos and P. Segers (2017). "Angiotensin II infusion into ApoE-/- mice: a model for aortic dissection rather than abdominal aortic aneurysm?" Cardiovasc Res 113(10): 1230-1242.

Trachet, B., A. Piersigilli, R. A. Fraga-Silva, L. Aslanidou, J. Sordet-Dessimoz, A. Astolfo, M. F. Stampanoni, P. Segers and N. Stergiopulos (2016). "Ascending Aortic Aneurysm in Angiotensin II-Infused Mice: Formation, Progression, and the Role of Focal Dissections." Arterioscler Thromb Vasc Biol 36(4): 673-681.

Tsamis, A., J. T. Krawiec and D. A. Vorp (2013). "Elastin and collagen fibre microstructure of the human aorta in ageing and disease: a review." J R Soc Interface 10(83): 20121004.

Tse, Z. T., H. Janssen, A. Hamed, M. Ristic, I. Young and M. Lamperth (2009). "Magnetic resonance elastography hardware design: a survey." Proc Inst Mech Eng H 223(4): 497-514.

Tsuruda, T., J. Kato, K. Hatakeyama, K. Kojima, M. Yano, Y. Yano, K. Nakamura, F. Nakamura-Uchiyama, Y. Matsushima, T. Imamura, T. Onitsuka, Y. Asada, Y. Nawa, T. Eto and K. Kitamura (2008). "Adventitial mast cells contribute to pathogenesis in the progression of abdominal aortic aneurysm." Circ Res 102(11): 1368-1377.

Turner, G. H., A. R. Olzinski, R. E. Bernard, K. Aravindhan, R. J. Boyle, M. J. Newman, S. D. Gardner, R. N. Willette, P. J. Gough and B. M. Jucker (2009). "Assessment of macrophage infiltration in a murine model of abdominal aortic aneurysm." J Magn Reson Imaging 30(2): 455-460.

Tzschatzsch, H., J. Guo, F. Dittmann, S. Hirsch, E. Barnhill, K. Johrens, J. Braun and I. Sack (2016). "Tomoelastography by multifrequency wave number recovery from time-harmonic propagating shear waves." Med Image Anal 30: 1-10.

Ulug, P., J. T. Powell, M. J. Sweeting, M. J. Bown, S. G. Thompson and S. C. Group (2016). "Meta-analysis of the current prevalence of screen-detected abdominal aortic aneurysm in women." Br J Surg 103(9): 1097-1104.

van Geuns, R.-J. M., P. A. Wielopolski, H. G. de Bruin, B. J. Rensing, P. M. A. van Ooijen, M. Hulshoff, M. Oudkerk and P. J. de Feyter (1999). "Basic principles of magnetic resonance imaging☆." Progress in Cardiovascular Diseases 42(2): 149-156.

Verzijl, N., J. DeGroot, S. R. Thorpe, R. A. Bank, J. N. Shaw, T. J. Lyons, J. W. Bijlsma, F. P. Lafeber, J. W. Baynes and J. M. TeKoppele (2000). "Effect of collagen turnover on the accumulation of advanced glycation end products." J Biol Chem 275(50): 39027-39031.

Vogel, P., S. Lother, M. A. Ruckert, W. H. Kullmann, P. M. Jakob, F. Fidler and V. C. Behr (2014). "MRI Meets MPI: a bimodal MPI-MRI tomograph." IEEE Trans Med Imaging 33(10): 1954-1959.

Wagenseil, J. E. and R. P. Mecham (2009). "Vascular extracellular matrix and arterial mechanics." Physiol Rev 89(3): 957-989.

Wagenseil, J. E. and R. P. Mecham (2012). "Elastin in large artery stiffness and hypertension." J Cardiovasc Transl Res 5(3): 264-273.

Wahlgren, C. M., E. Larsson, P. K. Magnusson, R. Hultgren and J. Swedenborg (2010). "Genetic and environmental contributions to abdominal aortic aneurysm development in a twin population." J Vasc Surg 51(1): 3-7; discussion 7.

Wang, S., C. Zhang, M. Zhang, B. Liang, H. Zhu, J. Lee, B. Viollet, L. Xia, Y. Zhang and M. H. Zou (2012). "Activation of AMP-activated protein kinase alpha2 by nicotine instigates formation of abdominal aortic aneurysms in mice in vivo." Nat Med 18(6): 902-910.

Wang, Z., J. Guo, X. Han, M. Xue, W. Wang, L. Mi, Y. Sheng, C. Ma, J. Wu and X. Wu (2019). "Metformin represses the pathophysiology of AAA by suppressing the activation of PI3K/AKT/mTOR/autophagy pathway in ApoE(-/-) mice." Cell Biosci 9: 68.

Wanhainen, A., F. Verzini, I. Van Herzeele, E. Allaire, M. Bown, T. Cohnert, F. Dick, J. van Herwaarden, C. Karkos, M. Koelemay, T. Kolbel, I. Loftus, K. Mani, G. Melissano, J. Powell, Z. Szeberin, C. Esvs Guidelines, G. J. de Borst, N. Chakfe, S. Debus, R. Hinchliffe, S. Kakkos, I. Koncar, P. Kolh, J. S. Lindholt, M. de Vega, F. Vermassen, R. Document, M. Bjorck, S. Cheng, R. Dalman, L. Davidovic, K. Donas, J. Earnshaw, H. H. Eckstein, J. Golledge, S. Haulon, T. Mastracci, R. Naylor, J. B. Ricco and H. Verhagen (2019). "Editor's Choice - European Society for Vascular Surgery (ESVS) 2019 Clinical Practice Guidelines on the Management of Abdominal Aorto-iliac Artery Aneurysms." Eur J Vasc Endovasc Surg 57(1): 8-93.

Ward, M. R., G. Pasterkamp, A. C. Yeung and C. Borst (2000). "Arterial remodeling. Mechanisms and clinical implications." Circulation 102(10): 1186-1191.

Weizenecker, J., B. Gleich, J. Rahmer, H. Dahnke and J. Borgert (2009). "Three-dimensional real-time in vivo magnetic particle imaging." Phys Med Biol 54(5): L1-L10.

Wicky, S., C. M. Fan, S. C. Geller, A. Greenfield, J. Santilli and A. C. Waltman (2003). "MR angiography of endoleak with inconclusive concomitant CT angiography." AJR Am J Roentgenol 181(3): 736-738.

Winlove, C. P., K. H. Parker, N. C. Avery and A. J. Bailey (1996). "Interactions of elastin and aorta with sugars in vitro and their effects on biochemical and physical properties." Diabetologia 39(10): 1131-1139.

Wu, K., D. Su, R. Saha, J. Liu, V. K. Chugh and J.-P. Wang (2020). "Magnetic Particle Spectroscopy: A Short Review of Applications Using Magnetic Nanoparticles." ACS Applied Nano Materials 3(6): 4972-4989.

Wu, L. C., Y. Zhang, G. Steinberg, H. Qu, S. Huang, M. Cheng, T. Bliss, F. Du, J. Rao, G. Song, L. Pisani, T. Doyle, S. Conolly, K. Krishnan, G. Grant and M. Wintermark (2019). "A Review of Magnetic Particle Imaging and Perspectives on Neuroimaging." AJNR Am J Neuroradiol 40(2): 206-212.

Xu, C., C. K. Zarins and S. Glagov (2001). "Aneurysmal and occlusive atherosclerosis of the human abdominal aorta." J Vasc Surg 33(1): 91-96.

Xu, L., J. Chen, K. J. Glaser, M. Yin, P. J. Rossman and R. L. Ehman (2013). "MR elastography of the human abdominal aorta: a preliminary study." J Magn Reson Imaging 38(6): 1549-1553.

Yacoub, E., M. D. Grier, E. J. Auerbach, R. L. Lagore, N. Harel, G. Adriany, A. Zilverstand, B. Y. Hayden, S. R. Heilbronner, K. Ugurbil and J. Zimmermann (2020). "Ultra-high field (10.5 T) resting state fMRI in the macaque." Neuroimage 223: 117349.

Yao, L., A. R. Folsom, A. Alonso, P. L. Lutsey, J. S. Pankow, W. Guan, S. Cheng, F. A. Lederle and W. Tang (2018). "Association of carotid atherosclerosis and stiffness with abdominal aortic aneurysm: The atherosclerosis risk in communities (ARIC) study." Atherosclerosis 270: 110-116.

Yoon, H., H. J. Shin, M. J. Kim, S. J. Han, H. Koh, S. Kim and M. J. Lee (2019). "Predicting gastroesophageal varices through spleen magnetic resonance elastography in pediatric liver fibrosis." World J Gastroenterol 25(3): 367-377.

Zdun, L. and C. Brandt (2021). "Fast MPI reconstruction with non-smooth priors by stochastic optimization and data-driven splitting." Phys Med Biol 66(17).

Zhang, L., X. Long, M. Nijiati, T. Zhang, M. Li, Y. Deng, S. Kuang, Y. Xiao, J. Zhu, B. He, J. Chen, P. Rossman, K. J. Glaser, S. K. Venkatesh, R. L. Ehman and J. Wang (2021). "Tumor stiffness measured by 3D magnetic resonance elastography can help predict the aggressiveness of endometrial carcinoma: preliminary findings." Cancer Imaging 21(1): 50.

Zhang, X., X. Zhu, C. M. Ferguson, K. Jiang, T. Burningham, A. Lerman and L. O. Lerman (2018). "Magnetic resonance elastography can monitor changes in medullary stiffness in response to treatment in the swine ischemic kidney." MAGMA 31(3): 375-382.

Zhou, H. F., H. Yan, J. L. Cannon, L. E. Springer, J. M. Green and C. T. Pham (2013). "CD43-mediated IFN-gamma production by CD8+ T cells promotes abdominal aortic aneurysm in mice." J Immunol 190(10): 5078-5085.

Zhou, X. Y., Z. W. Tay, P. Chandrasekharan, E. Y. Yu, D. W. Hensley, R. Orendorff, K. E. Jeffris, D. Mai, B. Zheng, P. W. Goodwill and S. M. Conolly (2018). "Magnetic particle imaging for radiation-free, sensitive and high-contrast vascular imaging and cell tracking." Curr Opin Chem Biol 45: 131-138.

9 RELATED PUBLICATIONS

Adams LC, Brangsch J, Kaufmann JO, **Mangarova DB**, Moeckel J, Kader A, Buchholz R, Karst U, Botnar RM, Hamm B, Makowski MR, Keller S. Effect of Doxycycline on Survival in Abdominal Aortic Aneurysms in a Mouse Model. Contrast Media Mol Imaging. 2021 Apr 27;2021:9999847. doi: 10.1155/2021/9999847. PMID: 34007253; PMCID: PMC8099506.

Kader A, Brangsch J, Kaufmann JO, Zhao J, **Mangarova DB**, Moeckel J, Adams LC, Sack I, Taupitz M, Hamm B, Makowski MR. Molecular MR Imaging of Prostate Cancer. Biomedicines. 2020 Dec 22;9(1):1. doi: 10.3390/biomedicines9010001. PMID: 33375045; PMCID: PMC7822017.

Kader, A., Brangsch, J., Reimann, C., Kaufmann, J. O., **Mangarova, D. B**., Moeckel, J., Adams, L. C., Zhao, J., Saatz, J., Traub, H., Buchholz, R., Karst, U., Hamm, B., & Makowski, M. R. (2021). Visualization and Quantification of the Extracellular Matrix in Prostate Cancer Using an Elastin Specific Molecular Probe. Biology, 10(11), 1217. https://doi.org/10.3390/biology10111217

Kaufmann, J. O., Brangsch, J., Kader, A., Saatz, J., **Mangarova, D. B**., Zacharias, M., Kempf, W. E., Schwaar, T., Ponader, M., Adams, L. C., Möckel, J., Botnar, R. M., Taupitz, M., Mägdefessel, L., Traub, H., Hamm, B., Weller, M. G., & Makowski, M. R. (2022). ADAMTS4-specific MR probe to assess aortic aneurysms in vivo using synthetic peptide libraries. Nature communications, 13(1), 2867. https://doi.org/10.1038/s41467-022-30464-8

Mangarova DB, Brangsch J, Moeckel J, Kader A, Ludwig A, Hamm B, Makowski MR. Current trends in molecular magnetic resonance imaging of the extracellular matrix in atherosclerosis. J Transl Sci May 2020;7(1-4): doi: 10.15761/JTS.1000393

Mangarova DB, Brangsch J, Mohtashamdolatshahi A, Kosch O, Paysen H, Wiekhorst F, Klopfleisch R, Buchholz R, Karst U, Taupitz M, Schnorr J, Hamm B, Makowski MR. Ex vivo magnetic particle imaging of vascular inflammation in abdominal aortic aneurysm in a murine model. Sci Rep. 2020 Jul 24;10(1):12410. doi: 10.1038/s41598-020-69299-y. PMID: 32709967; PMCID: PMC7381631.

Mangarova DB. Magnetic particle imaging of vascular inflammation in abdominal aortic aneurysm in murine model. Poster session presented at: 10th International Workshop on Magnetic Particle Imaging, 2020 Sep 7-8; digital event.

Mangarova DB. MR Elastography of abdominal aortic aneurysm specimens. Poster session presented at: 10th International Workshop on Magnetic Particle Imaging, 2021 May 17; digital event.

Mangarova, D. B., Bertalan, G., Jordan, J., Brangsch, J., Kader, A., Möckel, J., Adams, L. C., Sack, I., Taupitz, M., Hamm, B., Braun, J., & Makowski, M. R. (2021). Microscopic multifrequency magnetic resonance elastography of ex vivo abdominal aortic aneurysms for extracellular matrix imaging in a mouse model. Acta biomaterialia, S1742-7061(21)00774-1. Advance online publication. https://doi.org/10.1016/j.actbio.2021.11.026

Möckel J, Brangsch J, Reimann C, Kaufmann JO, Sack I, **Mangarova DB**, Kader A, Taupitz M, Adams LC, Keller S, Ludwig A, Hamm B, Botnar RM, Makowski MR. Assessment of Albumin ECM Accumulation and Inflammation as Novel In Vivo Diagnostic Targets for Multi-Target MR Imaging. Biology (Basel). 2021 Sep 27;10(10):964. doi: 10.3390/biology10100964. PMID: 34681063; PMCID: PMC8533611.

Zhao J, Kader A, **Mangarova DB**, Brangsch J, Brenner W, Hamm B, Makowski MR. Dynamic Contrast-Enhanced MRI of Prostate Lesions of Simultaneous [^{68}Ga]Ga-PSMA-11 PET/MRI: Comparison between Intraprostatic Lesions and Correlation between Perfusion Parameters. Cancers (Basel). 2021 Mar 19;13(6):1404. doi: 10.3390/cancers13061404. PMID: 33808685; PMCID: PMC8003484.

Zhao J, **Mangarova DB**, Brangsch J, Kader A, Hamm B, Brenner W, Makowski MR. Correlation between Intraprostatic PSMA Uptake and MRI PI-RADS of [^{68}Ga]Ga-PSMA-11 PET/MRI in Patients with Prostate Cancer: Comparison of PI-RADS Version 2.0 and PI-RADS Version 2.1. Cancers (Basel). 2020 Nov 26;12(12):3523. doi: 10.3390/cancers12123523. PMID: 33255971; PMCID: PMC7759872.

10 ACKNOWLEDGEMENTS

I would like to express my deep gratitude to everyone who supported me during the accomplishment of this doctorate program. My sincere thanks are given to Prof. Dr. Robert Klopfleisch for the supervision and guidance and to Prof. Dr. Marcus R. Makowski for the initiation of this project and continuous support.

This dissertation would not have been possible without the assistance of my fellow researchers. I am truly thankful to my colleagues from the AG Makowski group – Dr. Lisa Adams, Dr. Julia Brangsch, Jennifer Heyl, Avan Kader, Jan Ole Kaufmann and Jana Möckel for the great team spirit and constant encouragement. Special recognition goes to our SFB 1340 cooperation partners from the AG Experimental Radiology group, AG Elastography group, Physikalisch-Technische Bundesanstalt and Technische Universität Münster, especially to Dr. Jürgen Braun, Jakob Jordan, Dr. Azadeh Mohtashamdoltshahi and Dr. Olaf Kosch for their substantial assistance and guidance throughout the imaging measurements.

Finally, I would like to thank my loved ones for their moral support and for proofreading this work as well as my family for always letting me chase my dreams and goals.

11 SOURCES OF FUNDING

This work was funded by the Deutsche Forschungsgemeinschaft (DFG, German Research Foundation) – Project number 372486779 - SFB 1340, B01, MA 5943/3-1/4-1/9-1.

12 CONFLICTS OF INTEREST

The author has no conflicts of interest to declare.

13 SELBSTSTÄNDIGKEITSERKLÄRUNG

Hiermit bestätige ich, dass ich die vorliegende Arbeit selbstständig angefertigt habe. Ich versichere, dass ich ausschließlich die angegebenen Quellen und Hilfen in Anspruch genommen habe.

Hereby, I declare that I have composed the presented dissertation independently on my own and without any other resources than the ones indicated.

Berlin, den 05.04.2022 Dilyana Mangarova

Druck: mbvberlin mensch und buch verlag